Development/Plasticity/Repair

A Serotonin Circuit Acts as an Environmental Sensor to Mediate Midline Axon Crossing through EphrinB2

Lingyan Xing,[1,2,3] Jong-Hyun Son,[2,3] Tamara J. Stevenson,[2,3] Christina Lillesaar,[4,5] Laure Bally-Cuif,[5] Tiffanie Dahl,[1,3] and Joshua L. Bonkowsky[1,2,3]

[1]Interdepartmental Program in Neurosciences, [2]Department of Pediatrics, and [3]Department of Neurobiology and Anatomy, University of Utah School of Medicine, Salt Lake City, Utah 84108, [4]Department of Physiological Chemistry, Würzburg University, 97074 Würzburg, Germany, and [5]Laboratory of Neurobiology and Development, Centre National de la Recherche Scientifique Institute of Neurobiology Alfred Fessard, 91190 Gif-sur-Yvette cedex, France

Modulation of connectivity formation in the developing brain in response to external stimuli is poorly understood. Here, we show that the raphe nucleus and its serotonergic projections regulate pathfinding of commissural axons in zebrafish. We found that the raphe neurons extend projections toward midline-crossing axons and that when serotonergic signaling is blocked by pharmacological inhibition or by raphe neuron ablation, commissural pathfinding is disrupted. We demonstrate that the serotonin receptor *htr2a* is expressed on these commissural axons and that genetic knock-down of *htr2a* disrupts crossing. We further show that knock-down of *htr2a* or ablation of the raphe neurons increases ephrinB2a protein levels in commissural axons. An *ephrinB2a* mutant can rescue midline crossing when serotonergic signaling is blocked. Furthermore, we found that regulation of serotonin expression in the raphe neurons is modulated in response to the developmental environment. Hypoxia causes the raphe to decrease serotonin levels, leading to a reduction in midline crossing. Increasing serotonin in the setting of hypoxia restored midline crossing. Our findings demonstrate an instructive role for serotonin in axon guidance acting through *ephrinB2a* and reveal a novel mechanism for developmental interpretation of the environmental milieu in the generation of mature neural circuitry.

Key words: **axon guidance; connectivity; hypoxia; pathfinding; serotonin; zebrafish**

Significance Statement

We show here that serotonin has a novel role in regulating connectivity in response to the developmental environment. We demonstrate that serotonergic projections from raphe neurons regulate pathfinding of crossing axons. The neurons modulate their serotonin levels, and thus alter crossing, in response to the developmental environment including hypoxia. The findings suggest that modification of the serotonergic system by early exposures may contribute to permanent CNS connectivity alterations. This has important ramifications because of the association between premature birth and accompanying hypoxia, and increased risk of autism and evidence associating *in utero* exposure to some antidepressants and neurodevelopmental disorders. Finally, this work demonstrates that the vertebrate CNS can modulate its connectivity in response to the external environment.

Introduction

Current models propose that neural circuitry development in the vertebrate brain is governed by an early-life genetic program that constrains the range of potential connectivity and behaviors but is then refined by experience-driven neuronal activity to refine this template (Katz and Shatz, 1996). Recent evidence also shows a role for neuronal activity in the development of normal connectivity (Hanson and Landmesser, 2004; Suárez et al., 2014). However, it is not known whether intrinsic mechanisms exist to modulate developing CNS connectivity in response to exogenous developmental or environmental cues.

In the adult CNS, the neurotransmitter serotonin (5-HT) is known to act as a molecular mediator of plasticity (Jitsuki et al., 2011; Celada et al., 2013). Intriguingly, in early development,

Received April 2, 2015; revised Sept. 17, 2015; accepted Sept. 28, 2015.

Author contributions: L.X., J.-H.S., T.J.S., and J.L.B. designed research; L.X., J.-H.S., T.J.S., T.D., and J.L.B. performed research; L.X., J.-H.S., T.J.S., C.L., L.B.-C., and J.L.B. contributed unpublished reagents/analytic tools; L.X., J.-H.S., T.J.S., and J.L.B. analyzed data; L.X. and J.L.B. wrote the paper.

This work was supported by the National Institutes of Health (Grant DP2 MH100008 and National Institute of Mental Health Grant R21 MH107039) and the March of Dimes (Research Grant to J.L.B.). We thank M. Bastiani, M. Deans, R. Dorsky, M. Vetter, F. Poulain, and members of the Bonkowsky laboratory for helpful comments; M. Gulbransen for assistance in specimen preparation; T. Dahlem and the University of Utah Mutation Generation and Detection Core for CRISPR generation; and H. Burgess and A. Suli for sharing plasmids.

The authors declare no competing financial interests.

Correspondence should be addressed to Joshua L. Bonkowsky, 401 MREB, University of Utah, 20 North 1900 East, Salt Lake City, UT 84132. E-mail: joshua.bonkowsky@hsc.utah.edu.

DOI:10.1523/JNEUROSCI.1295-15.2015
 0270-6474/15/3514794-15$15.00/0

5-HT neurons and their axon projections are widespread in the vertebrate CNS. Projections from the 5-HT raphe nuclei (nuclei B1–B9) (Dahlström and Fuxe, 1964) arborize throughout the CNS (Steinbusch, 1981), including ascending projections in the telencephalon and descending innervation of the brainstem and spinal cord. Innervation occurs early in development (Rubenstein, 1998; Lillesaar et al., 2009), before the development of behaviors requiring 5-HT and before 5-HT's roles in the refinement of sensory maps (Lesch and Waider, 2012; Toda et al., 2013).

These findings suggest a nonclassical role for 5-HT in early development. Recent work has shown that 5-HT is necessary for neuron migration, dendrite arborization, and synapse formation (Persico et al., 2001; Matsukawa et al., 2003; Vitalis et al., 2007; Riccio et al., 2009). A potential role in pathfinding has also been observed. In mouse thalamocortical neuron explants, 5-HT caused a repulsive response to netrin-1 and overexpression of the 5-HT receptor *htr1B/1D* caused dorsoventral shifting of the axon tracts (Bonnin et al., 2007). In rat raphe neuron explants, knockdown of the 5-HT transporter caused altered fasciculation and projections of axons (Witteveen et al., 2013).

Precise mechanisms and roles for 5-HT in pathfinding are poorly understood. Is 5-HT a modulator to fine-tuning axon guidance or does it play a more instructive role in pathway choice? Because 5-HT signaling activates second messenger systems, how is specificity of action achieved? 5-HT has been shown in *Aplysia* to increase expression of neurexin and neuroligin at the synapse by increased kinesin-mediated transport (Puthanveettil et al., 2008; Choi et al., 2011), supporting the possibility of a role for 5-HT in regulating cell-surface receptors responsible for axon guidance.

Another unresolved feature is whether neural connectivity in vertebrates can be modulated during development, for example, by changes in 5-HT. Altered behavior in *C. elegans* can be caused by changes in 5-HT expression from environmental manipulation, apparently by alterations in neuropeptide and receptor expression in an extant neural circuit (Pocock and Hobert, 2010). In vertebrates, no similar mechanism has been noted. A role for 5-HT in interpreting exogenous stimuli and altering neural circuits during development would represent an unexpected means for altering an organism's neurobehavioral repertoire in response to parental or developmental exposures.

To investigate a role for 5-HT in neural circuit development, we applied the experimental tractability of the small vertebrate zebrafish (*Danio rerio*) to visualize axon guidance decisions. Here, we report that pharmacological blockade of 5-HT signaling, genetic ablation of the raphe neurons, or knock-down of 5-HT receptors leads to failure of midline axon crossing of telencephalic neurons. We further demonstrate that 5-HT's axon guidance role is mediated by downregulation of *ephrinB2a* (*efnB2a*) levels because loss of 5-HT signaling led to increased *efnB2a* levels, which caused failure of commissural axons to cross the midline. 5-HT expression is decreased by hypoxia; restoration of serotonergic signaling rescued hypoxic-mediated disruption of midline axon crossing. Our results show that raphe 5-HT neurons act as a sensor to alterations in the developmental milieu and their projections regulate pathfinding of a separate circuit. Therefore, our study demonstrates an instructive role for 5-HT in axon pathfinding and identifies a novel mechanism of connectivity development in the CNS.

Materials and Methods

Ethics statement. All zebrafish experiments were performed in accordance with guidelines from the University of Utah Institutional Animal Care and Use Committee regulated under federal law (the Animal Welfare Act and Public Health Services Regulation Act) by the U.S. Department of Agriculture and the Office of Laboratory Animal Welfare at the National Institutes of Health and accredited by the Association for Assessment and Accreditation of Laboratory Care International.

Fish stocks and animal husbandry. Adult fish were bred according to standard methods. Embryos were raised at 28.5°C in E3 embryo medium with methylene blue and embryos beyond 24 h postfertilization (hpf) were treated with phenylthiourea (PTU) to prevent pigment formation. Animals of either sex were used for experiments. For *in situ* staining and immunohistochemistry, embryos were fixed in 4% paraformaldehyde (PFA) in phosphate-buffered saline (PBS) overnight at 4°C, washed briefly in PBS with 0.1% Tween 20, dehydrated stepwise in methanol (MeOH) (25%, 50%, 75%, 100%), and stored in 100% MeOH at −20°C until use.

Transgenic fish lines, and alleles used were the following: Tg(*foxP2-enhancerA.2:egfp-caax*)^{zc69} (Stevenson et al., 2012); Tg(*foxP2-enhancerA.2:Gal4-VP16*$_{413-470}$)^{zc72} (Stevenson et al., 2012); Tg(*myl7:EGFP*; *UAS:TagRFP-caax*)^{zc61}; *efnb2a*$^{hu3393/+}$ (Kettleborough et al., 2013; http://www.sanger.ac.uk/sanger/Zebrafish_Zmpgene/ENSDARG00000020164#hu3393); Tg(*UAS:Eco.NfsB-mCherry*)^{rw0144} (referred to as Tg(*UAS:NTR-mCherry*)) (Davison et al., 2007); Tg(*tph2:GAL4FF*)^{y228Tg} (Yokogawa et al., 2012); Tg(*fev:GAL4-GFP*)^{gy1} (generated from the −*3.2pet1* enhancer, Lillesaar et al., 2009). Lines are available from the Zebrafish International Resource Center or upon request.

Hypoxia reagents. For induction and monitoring of hypoxia, embryonic zebrafish were placed in a sealed Plexiglas chamber connected via a controller that monitored and adjusted nitrogen gas flow to a desired pO_2 set point (Biospherix) using previously established protocols (Stevenson et al., 2012). Embryos were incubated in 1% O_2 from 24 to 36 hpf. Morphological staging was used to determine age at fixation for analysis.

Scoring tract of the commissure of the posterior tuberculum axon errors, C/L1 and C/L2 intensity ratios, and anterior commissure. Evaluation of tract of the commissure of the posterior tuberculum (TCPT) midline axon crossing defects was determined as described previously (Stevenson et al., 2012) with the following modifications: we measured the total fluorescence intensity (average intensity × area) of a rectangular area placed over the commissure or longitudinal tract. The rectangle (set size, 10 × 30 pixels in ImageJ) was placed over the midline of the commissural TCPT (TCPTc) pathway or over the longitudinal axons immediately rostral to (L1) or caudal to (L2) their decussation into the TCPT. A confocal *z*-stack of 10 slices (step size 2 μm) was taken of the region using identical confocal settings (20× objective, PMT range 400–600, imaging speed 12.5 μs/pixel) and then the fluorescence of the average intensity projection was calculated. A ratio of the commissural versus longitudinal axon intensity was calculated (C/L1, C/L2 ratio; see Fig. 2*H*). Some experimental variation was noted, so results were only compared directly for experiments performed on the same day.

To assess whether crossing was affected in the anterior commissure by ketanserin, we visualized and imaged Tg(*foxP2-enhancerA.2:egfp-caax*) embryos and made average intensity projections of *z*-slices starting at the equator of the lens and then extending five steps dorsally (six *z*-slices total; step size 2 μm). We then calculated the area of the anterior commissure and its average fluorescence intensity.

Immunohistochemistry and in situ *hybridization*. Immunohistochemistry was performed as described previously (Bonkowsky et al., 2008; Stevenson et al., 2012; Xing et al., 2012). Antibodies used were as follows: mouse anti-tubulin 1:250 (Developmental Studies Hybridoma Bank, 6G7), mouse monoclonal α-GFP 1:250 (Millipore, MAB3580), goat polyclonal α-ephrinB2a 1:20 (R&D Systems, AF1088), rabbit α-serotonin 1:500 (ImmunoStar, 20080), mouse α-HuC/D 1:250 (Invitrogen, A21271), rabbit α-TagRFP 1:250 (Evrogen, AB234), Cy-3 α-rabbit 1:400 (Millipore, AP132C), Alexa Fluor 488 donkey α-mouse 1:400 (Invitrogen, A21202), and Alexa Fluor 555 rabbit α-goat 1:100 (Invitrogen, A21429).

Tubulin immunohistochemistry was performed by fixation in 2% trichloroacetic acid overnight at 4°C. Embryos were washed with PBST 4 times for 5 min each, blocked for 1 h (Roche Western blocking reagent, 11921673001), and incubated with mouse anti-acetylated tubulin overnight at 4°C. After PBST washes, embryos were incubated with Alexa Fluor 488 donkey α-mouse overnight at 4°C.

Quantification of 5-HT in hypoxia/normoxia. Images were obtained with identical confocal settings for all embryos. Intensities were calculated in a rectangle of set size (70 × 100 pixels in ImageJ) placed over the raphe nuclei (rostral edge of the rectangle was placed at the rostral-most 5-HT raphe neurons) using average intensity projections of 5 *z*-slices (step size 2 μm). HuC/D intensity was also measured with the same *z* projections. 5-HT intensity level was normalized to HuC/D.

Quantification of ephrinB2a levels. α-ephrinB2a staining intensity was determined in control and ketanserin-treated embryos at 36 hpf and in control and metronidazole (Mtz)-treated embryos at 64 hpf; confocal images were obtained with identical confocal settings. Intensities were calculated in rectangles of fixed size in control/ketanserin over the telencephalon (78 × 72 pixels), diencephalon (24 × 50 pixels), or lens (74 × 107 pixels) using average intensity projections of 11 *z*-slices starting at the equator of the lens and then extending 5 steps dorsally and ventrally (11 *z*-slices total; step size 2 μm). In control/Mtz, rectangles were over the telencephalon (85 × 110 pixels), diencephalon (34 × 64 pixels), and lens (105 × 165 pixels) using average intensity projections of 5 *z*-slices (5 slices from ventral-most edge of the lens; step size 2 μm). For quantification in TCPTc axons (see Fig. 8) at 36 hpf, a confocal projection over the diencephalon where the TCPT axons cross was performed with a total of 6 slices starting from the equator of the lens and moving dorsally with a step size of 2 μm. TCPTc staining intensity was normalized to that of the eye. The area of data collection was as follows: diencephalon (24 × 50 pixels), eye (74 × 107 pixels).

Western blot analysis. Western blotting was performed as described previously (Link et al., 2006) with the following modifications. Dechorionated and deyolked embryos at 48 hpf were homogenized in cold lysis buffer with protease inhibitors and samples were centrifuged at 4°C for 10 min. Supernatants were transferred to new microcentrifuge tubes and an equal volume of 2× Laemmli sample buffer was added. Samples were heated at 95°C for 3 min and then subjected to SDS-PAGE electrophoresis on a 4–20% gradient gel and blotted onto a PVDF membrane. Affinity-purified goat anti-ephrinB2a antibody (R&D Systems, AF1088) was applied at a 1:50 dilution and donkey anti-goat IgG-HRP (Pierce, PA1–28805) was applied at 1:2000. An identical blot was probed with mouse anti-α tubulin at a 1:5000 dilution (Sigma-Aldrich, T9026), and goat anti-mouse IgG-HRP at 1:5000 (Pierce, 1858413). The secondary antibody was visualized with an ECL reaction (GE LifeSciences) using standard protocols.

In situ *hybridization*. Antisense digoxigenin-labeled RNA probes were prepared for *tph2* (ENSDARG00000057239), *htr2ab* (ENSDARG00000058165), *htr2aa* (ENSDARG00000057029), and *htr2c* (ENSDARG00000018228) using standard methods (Bonkowsky and Chien, 2005). Probe for *tph2* was made from *pCR2.1TOPO z tphR* (*tph2*) D75 (from L. Bally-Cuif) and for *netrin1a* from *pBS-ntn1a* (from A. Suli) (Suli et al., 2006). To generate the *htr2ab*, *htr2aa*, and *htr2c* probes, cDNA from 3 dpf larvae was amplified with primers as follows: *htr2ab*, forward: 5′-GCAATGGGAGCGAAGAGAGA-3′; reverse: 5′-GGCCAGGTGTAACCGTAGAG-3′. *htr2aa*, forward: 5′-TCACACCTCCTTTTGGACGG-3′; reverse: 5′-TTAGCATTGCACGCATTCGG-3′; *htr2c*, forward: 5′-TAGACCTCGTTGGCTGGATG-3′; reverse: 5′-CACTAGAATCAGCAGGGCCG-3′. After gel purification, the fragment was cloned into pCR4-TOPO TA (Invitrogen) and sequenced to confirm its identity. To make antisense probe, the construct was linearized with SpeI and transcription performed using T7 polymerase.

In situ *hybridization combined with immunohistochemistry on sections*. *In situ* hybridization was performed as described above. After the *in situ* was completed, embryos were sequentially transferred to 5%, 15%, and then 30% sucrose (in PBS). Embryos were then embedded in optimal cutting temperature compound (Tissue-TeK, 4583) using a dry ice ethanol bath, and stored at −80°C at least overnight. Then, 20 μm sections were cut for immunostaining. Sections were boiled for 20 min with citrate buffer (10 mM sodium citrate, 0.05% Tween 20, pH 6.0) for antigen retrieval and then blocked for 30 min in 1% BSA, 0.1% fish skin gelatin (Sigma-Aldrich, G7765), and 0.1% Tween 20 in PBS. The sections were incubated with primary antibody mouse α-GFP 1:100 at room temperature for 1 h. After washing of the primary antibody with PBS for 3 × 5 min, the secondary donkey α-mouse Alexa Fluor 488 (1:100) was incubated at room temperature for 1 h.

Sparse and ipsilateral neuron labeling. One-cell-stage embryos were coinjected with plasmids for *UAS:lyn-TagRFP* (Yokogawa et al., 2012) or *UAS:GFP-caax* and *foxP2-enhancerA.2:Gal4* (Stevenson et al., 2012). A total of 25 pg of each plasmid was injected per embryo.

Microscopy, image analysis, and movie analysis. Image acquisition and analysis were performed as described previously (Bonkowsky et al., 2008). For 3D images, confocal images were processed with FluoRender (Wan et al., 2012). Rendered images were exported as TIFFs and converted into avi files using ImageJ.

Morpholino injections and htr2ab *mRNA expression analysis*. One-cell-stage embryos were injected with 6 ng of *htr2aa*, 6 ng of *htr2ab*, or 2 ng of *htr2c* splice-blocking morpholino (Gene Tools). RT-PCR to test splice blocking of morpholinos was performed as described previously (Xing et al., 2012).

Sequences for the morpholinos were *htr2ab* mo:5′-ATGTAAAGAAACTCACCGTAGAGGA-3′ (targeting gene ENSDARG00000058165); *htr2aa* mo: 5′-TAACCTGAAGAGGAGATACACATGC-3′ (targeting gene ENSDARG00000057029); and *htr2c* mo: 5′-TCAAATCCGTGTTTCTCTGACCTAT-3′ (targeting gene ENSDARG00000018228). RT-PCR to test splice blocking of morpholinos was performed as described previously (Xing et al., 2012). Primers for testing *htr2ab* morpholino efficacy were used to amplify the region encompassing exons 1 and 3 (forward: 5′-ATGGATTGCAATGGGAGCGA-3′; reverse: 5′-GATGAGCGGGACGAAAAACG-3′).

TUNEL staining. Terminal deoxynucleotidyl transferase dUTP nick-end labeling (TUNEL) was performed on whole-mount larvae (ApopTag Fluorescein *In Situ* Apoptosis Detection Kit; Millipore) as described previously (Lambert et al., 2012).

Drug treatment. Embryos were manually dechorionated at 24 hpf. E3/PTU-containing solution was mixed with the respective compound: 500 μM ketanserin (Sigma-Aldrich, S006), 2 μM fluoxetine (Sigma-Aldrich, F132), or 200 μM methysergide (Sigma-Aldrich, M137). Embryos were incubated with the compound from 24 to 72 hpf. Fixation with 4% PFA occurred at 72 hpf.

Mtz (Sigma-Aldrich, M1547) was dissolved in 0.05% or 0.2% DMSO in standard E3/PTU-containing solution. Before 24 hpf, embryos were exposed to 5 mM Mtz in 0.2% DMSO. At 24 hpf, embryos were manually dechorionated and exposed to 5 mM Mtz in 0.05% DMSO from 24 to 96 hpf. Fixation with 4% PFA occurred at 96 hpf.

qRT-PCR. qRT-PCR for *tph2* was performed on 36 and 48 hpf embryos. Each reaction was performed in triplicate and the mean of replicates was calculated; results were normalized to the mRNA level of *tph2* in wild-type embryos with β-actin transcript levels as a control. qRT-PCR for *ephrinB2a* was performed on 48 hpf embryos. Primers for *tph2* were forward 5′-TTTGTGGAGGTTGCAATGAA-3′ and reverse 5′-CAGTCCAGCCAGGAAGTCTC-3′. Primers for β-actin were forward 5′-CTCTTCCAGCCTTCCTTCCT-3′ and reverse 5′-CACCGATCCAGACGGAGTAT-3′. qRT-PCR for *ephrinB2a* was performed on 48 hpf embryos. Primers for *ephrinB2a* were forward 5′-CCCTACCAGTTACCCTCCCA-3′ and reverse 5′-CTCTGAGCCGTTGTTGTTGC-3′.

htr2ab *CRISPR/Cas9*. One-cell stage embryos from a mating of Tg(*foxP2:egfp-caax*) outcrossed to wild-type were injected with 1 ng of Cas9 protein (PNA Bio, CP01) and 600 pg of *htr2ab* sgRNA (Jao et al., 2013). sgRNA was targeted to the following sequence in *htr2ab*: GGTCATAATCATCACCGTGA. sgRNA synthesis followed the protocol as described previously (Jao et al., 2013). Embryos were collected at 24 hpf for mutation analysis using PCR and high-resolution melt analysis (HRMA) (Xing et al., 2012; Xing et al., 2014).

Genomic DNA from 24 hpf embryos was prepared as follows: embryos were incubated with 30 μl of 50 mM NaOH at 95°C for 25 min and then cooled to 4°C; next, 3 μl of 1 M Tris-HCl, pH 8.0, was added. PCRs were performed in 96-well hard-shell plates (Bio-Rad) in 10 μl of volume: 4 μl of 2.5× LightScanner Master Mix (Idaho Technology), 5 pmol of each primer (forward primer: 5′-GTCCAGAAGAACTGGGTGGC-3′; reverse primer: 5′-CTGGTCATCATGGCGGTGAG-3′), and 3 μl of genomic DNA template extracted above. PCRs were covered with 30 μl of mineral oil. PCR conditions were as follows: 2 min at 95°C, followed by

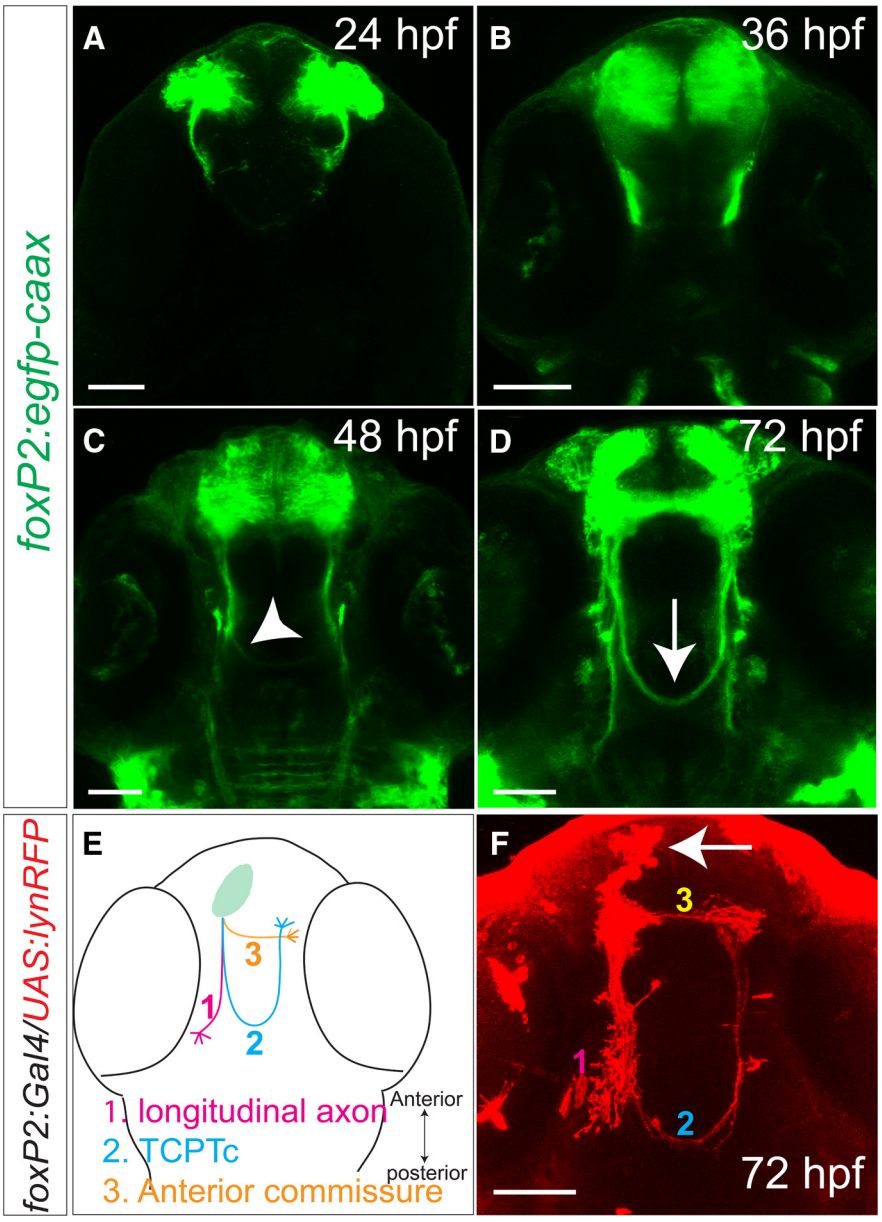

Figure 1. Axons labeled by *foxP2-enhancerA.2:egfp-caax* and the TCPT commissure. Confocal images of whole-mount embryos, rostral top. Scale bar, 50 μm. ***A–D***, Tg(*foxP2-enhancerA.2:egfp-caax*) embryos, maximum intensity *z*-stack projections, α-GFP immunohistochemistry. ***A–C***, Midline TCPTc axon crossing begins ~36–48 hpf (arrowhead). ***D***, By 72 hpf, the TCPTc is formed (arrow). ***E***, Schematic illustration of three major axon pathways of *foxP2-enhancerA.2* neurons: (1) longitudinal axons, (2) the TCPTc, and (3) the anterior commissure. ***F***, Projection targets of *foxP2* neurons were determined by sparse ipsilateral neuron labeling (arrow) using coinjection of plasmids carrying *UAS:lyn-TagRFP* and *foxP2-enhancerA.2:Gal4* at the one-cell stage stained for α-RFP. *foxP2* neurons project longitudinally, across the anterior commissure, or across the TCPTc.

28 cycles of 10 s at 95°C, 30 s at 68°C, ending with 95°C for 30 s and cooled to 15°C. HRMA was performed on a LightScanner-96 instrument (Idaho Technology) from 60°C to 97°C with a temperature transition rate of 0.1°C/s. For sequencing the targeted region in F0 founders, PCR amplicons were cloned into pCR4-TOPO TA (Invitrogen). Plasmids were isolated from individual colonies and Sanger sequenced.

5-HT HPLC-ECD in zebrafish larvae. 5-HT tissue content in zebrafish larvae was determined via high-pressure liquid chromatography system coupled to an electrochemical detector (HPLC-ECD) essentially as described previously (Son et al., 2011; McFadden et al., 2012). Embryos ($n = 100$ each condition; performed in triplicate) were collected at 48 hpf from normoxic or hypoxic conditions (1% O_2, 24–36 hpf). Embryos were sonicated in tissue buffer [0.05 M sodium phosphate/0.03 M citric acid, 25% methanol (v/v), pH 2.5] and centrifuged (22,000 × *g*) twice. Then, 25 μl of supernatant was injected onto an HPLC-ECD (EOx = +0.7 V; Decade, Antech). A Whatman PartiSphere C-18 column (250 × 4.6 mm, 5 μm; Whatman) and mobile phase [0.05 M sodium phosphate, 0.03 M citrate buffer, 0.1 M EDTA, MeOH (20% v/v), and 0.030–0.035% sodium octyl sulfate, pH 2.85, flow rate = 0.75 ml/min] were used to detect 5-HT. 5-HT tissue content was expressed per microgram of protein determined with a Pierce BCA Protein Assay Kit.

Results

5-HT blockade causes commissural axon pathfinding errors

To study the role of 5-HT in axon pathfinding, we used the transgenic line *Tg(foxP2-enhancerA.2:egfp-caax)*, which expresses membrane-targeted GFP in a subset of neurons in the telencephalon (Stevenson et al., 2012). Tg(*foxP2-enhancerA.2:egfp-caax*) neurons project axons in the anterior commissure, longitudinal pathways, and the TCPTc (Wilson et al., 1990). As we have reported previously (Stevenson et al., 2012), the TCPTc axons start to extend at 24 hpf. By 36–48 hpf, axons are preparing to cross the midline; most axons have crossed by 72 hpf and the commissure is fully formed by 96 hpf (Fig. 1*A–D*). To clarify the targets and pathways of these axons, we performed ipsilateral sparse labeling of the neurons labeled by *foxP2-enhancerA.2* by transient expression of coinjected plasmids *foxP2-enhancerA.2:Gal4* and *UAS:lyn-TagRFP* (Stevenson et al., 2012; Yokogawa et al., 2012) into one-cell-stage embryos. We observed three different projection classes: a subset of axons that cross the midline as the TCPTc and target onto the contralateral neurons in the telencephalon, a subset that extends longitudinally into the caudal diencephalon, and axons that cross directly in the anterior commissure onto neurons in the contralateral telencephalon (Fig. 1*E*,*F*).

To test the effects of 5-HT on axon pathfinding, we tried a variety of pharmacological manipulations of 5-HT signaling. Embryos were dechorionated and incubated with different compounds from 24 to 72 hpf during the critical period for *foxP2-enhancerA.2* axon pathfinding. The nonspecific 5-HT receptor antagonist methysergide (Silberstein, 1998) caused defects in midline crossing of the TCPTc, but the overall health of the embryos was compromised and it was unclear whether the pathfinding errors were a secondary nonspecific effect. When we incubated embryos with the 5-HT receptor type 2 (hydroxytryptamine receptor 2, htr2) antagonist ketanserin (Brogden and Sorkin, 1990), there was no effect on overall mortality or development of the embryos. However, Tg(*foxP2-enhancerA.2:egfp-caax*) embryos treated with ketanserin had failure to form the TCPTc or a reduction in the number of TCPTc axons crossing the midline (Fig. 2*A*,*B*).

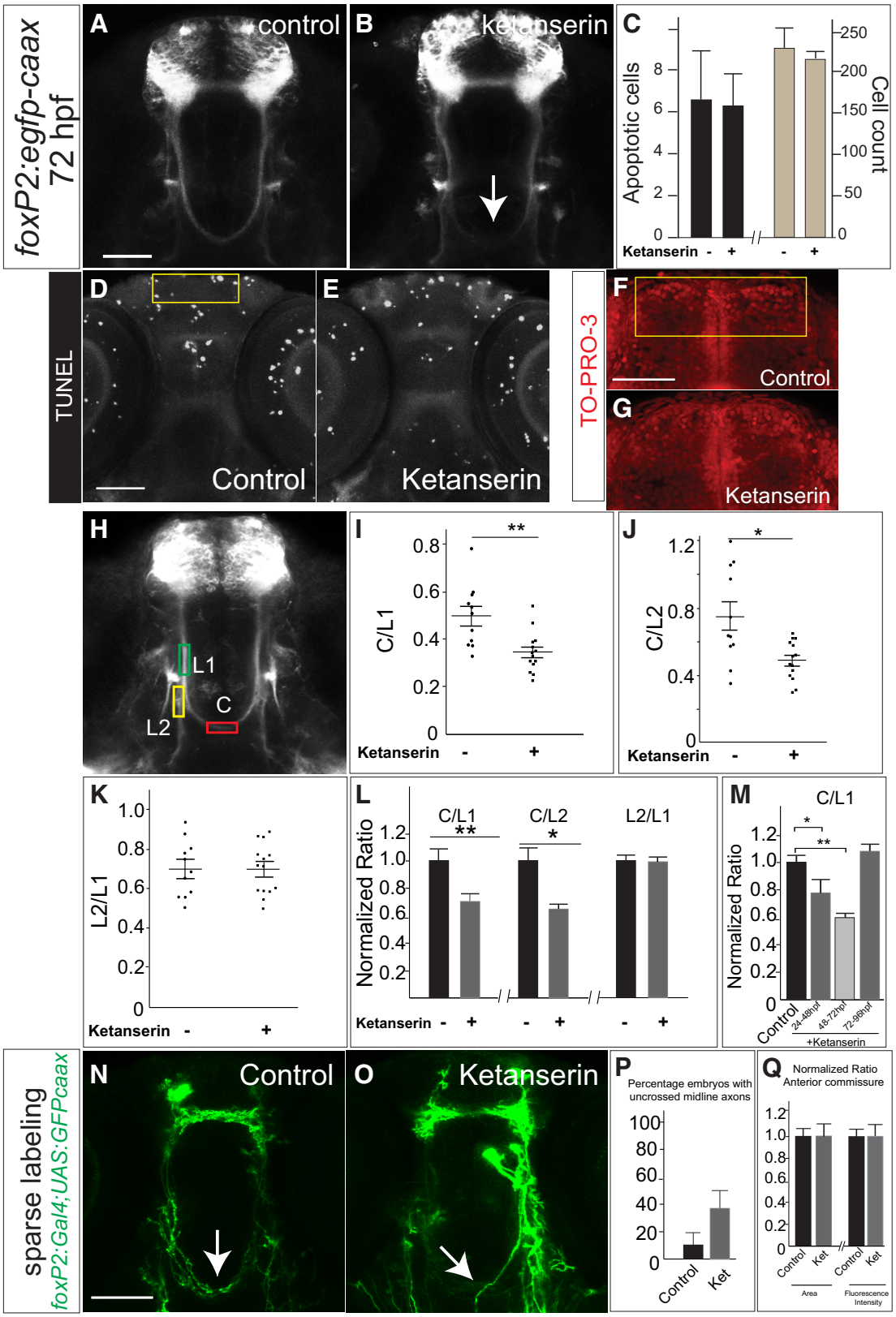

Figure 2. Commissural axon projections of TCPT neurons are disrupted by blockade of 5-HT signaling. ***A***, ***B***, Tg(*foxP2-enhancerA.2:egfp-caax*) embryos, maximum intensity *z*-stack projections, α-GFP immunohistochemistry, rostral top. Scale bar, 50 μm. TCPTc midline axon crossing is disrupted (arrow) when treated with ketanserin (***B***) compared with control (***A***). ***C***, Ketanserin does not cause increased apoptosis in treated embryos or changes in overall cell counts in the telencephalon, $n = 5$ each group. Error bars indicate SD (apoptosis) or SEM (cell counts). ***D***, ***E***, Representative TUNEL images used for quantification, confocal *z*-stacks, rostral top, area for quantification in yellow box. Scale bar, 50 μm. ***F***, ***G***, Representative TO-PRO-3 staining in telencephalon, area for quantification in yellow box. Scale bar, 50 μm. ***H***, Confocal image of Tg(*foxP2-enhancerA.2:egfp-caax*) embryo showing where measurements were made for the intensity of commissural (C), precrossing longitudinal (L1), and postcrossing (L2) axon tracts (see Materials and Methods for details). ***I–K***, Scatterplots of results from individual embryos showing the distribution of C/L results. $n = 11$ and 14, respectively, in control and ketanserin-treated groups. $^*p < 0.05$, $^{**}p < 0.01$; Student's *t* test. Error bars indicate SEM. ***I***, ***J***, Results of ketanserin-treated (*Figure legend continues.*)

The effects of ketanserin were dose dependent: levels of 200 μM had minimal effect on TCTPc pathfinding (data not shown) and 500 μM was used for experiments. We did not observe any differences in apoptosis in control compared with ketanserin-treated embryos (Fig. 2*C–E*). Further, the reduction in crossing axons was not due to a loss of *foxP2* neurons because control and ketanserin-treated embryos had the same number of telencephalic neurons (Fig. 2*C*,*G*). We noted that the defects in axon guidance persisted at 5 dpf, indicating that the pathfinding errors were not due to a developmental delay.

To quantify the changes in commissure axon crossing, we calculated fluorescence intensity ratios of commissure to longitudinal axons (C/L ratios, Stevenson et al., 2012). Effects of ketanserin on the TCPTc ranged from minimal to complete loss of the TCPTc and varied from embryo to embryo. We measured the signal intensity of the commissure axons compared with the precommissure longitudinal tract axons (C/L1 ratio) and with the postcommissure longitudinal tract axons (C/L2 ratio) (Fig. 2*H–L*). A lower C/L ratio indicates fewer TCPTc axons crossing the midline. Finally, we also compared the intensity of the precommissure longitudinal tract with the postcommissure longitudinal tract in control and ketanserin-treated embryos (L2/L1 ratio; Fig. 2*K*). We reasoned that, if axons in ketanserin-treated embryos were indeed aberrantly selecting the longitudinal pathway in preference to the TCPTc, we would see an increase of L2/L1 in treated embryos. To address this, we examined individual embryo raw data ratios, which are shown as scatterplots (Fig. 2*I–K*), as well as normalized ratios (Fig. 2*L*). We found that embryos treated with ketanserin had both decreased C/L1 and C/L2 ratios (Fig. 2*I*,*K*), which is consistent with the decrease in axons crossing the TCPTc. In addition, in ketanserin-treated embryos, the L2/L1 ratio did not change (Fig. 2*K*), suggesting that axons did not select the L2 longitudinal tract preferentially. The effect of ketanserin was developmentally restricted: the maximal effect of ketanserin was seen by exposure from 48 to 72 hpf, consistent with the timing when most of the TCPTc axons cross the midline, whereas embryos incubated in ketanserin from 72 to 96 hpf did not have disrupted midline crossing (Fig. 2*M*).

To further confirm that blockade of serotonin specifically caused a change in midline axon crossing fluorescence intensity due to errors in pathfinding, we performed sparse labeling of individual or small groups of neurons by coinjecting plasmids to label the TCPTc (Fig. 2*N*,*O*). We found that ketanserin caused an increase in the percentage of axons that failed to cross the midline (Fig. 2*P*), consistent with the C/L ratio measurements. We also tested whether ketanserin affected other axon tracts by measuring both the area and fluorescence intensity of the anterior commissure in Tg(*foxP2-enhancerA.2:egfp-caax*) embryos. We did not find any change in the anterior commissure by serotonin blockade (Fig. 2*Q*), although it is possible that smaller changes in crossing could be masked by the larger number of axons crossing in the anterior commissure.

5-HT receptors are necessary for commissural axon crossing

Because we noted the effect of blocking 5-HT signaling, in particular of the *htr2* antagonist ketanserin, on midline axon crossing, we next determined which *htr2* receptors were expressed in *foxP2* neurons. More than 14 different 5-HT receptors are expressed in the vertebrate CNS (Barnes and Sharp, 1999). Ketanserin has high affinity for serotonin type 2A receptors, but can also bind with lower affinity to type 2C receptors (Saxena, 1995). Expression of *htr2aa*, *htr2ab*, and *htr2c* in the 48 hpf zebrafish CNS exhibit a spatial overlap in the telencephalon with *foxP2* neurons (Schneider et al., 2012). We used sections of *Tg*(*foxP2-enhancerA.2:egfp-caax*) embryos to perform double staining with immunohistochemistry for GFP and *in situ* hybridization for *htr2aa*, *htr2ab*, or *htr2c*. We found that all three receptors were coexpressed in *foxP2* neurons, as well as in *foxP2* axons as they extend caudally to form the TCPTc. As explained below, we focused our analysis on *htr2ab* (Fig. 3*A*,*B′′*).

To demonstrate the necessity of *htr2* for TCPTc axon guidance and to determine which receptor subtype(s) were involved, we used morpholino knock-down of the different *htr2* receptors alone and in combination. Knock-down of *htr2aa* or *htr2c* did not affect the TPCTc (Fig. 3*F*,*G*). However, knock-down of *htr2ab* led to a reduction in the C/L1 ratio of the TCPTc, suggesting that 5-HT signaling via *htr2ab* receptors is critical for axon midline crossing (Fig. 3*C*,*E*,*G*). Because there was still some crossing of the TCPTc, we tried coinjection of *htr2ab* and *htr2aa* morpholinos. This caused disruption of embryogenesis and severe dysmorphism of the body axis, preventing analysis of pathfinding.

To confirm specificity of the *htr2ab* morpholino phenotype, we designed and used CRISPR/Cas9 gene disruption of *htr2ab* (Fig. 3*D*). Injection of CRISPR/Cas9 can lead to high-frequency biallelic disruption of the targeted gene in somatic cells (Jinek et al., 2012; Jao et al., 2013). We coinjected Cas9 protein and an *htr2ab* short guide RNA (sgRNA) into one-cell-stage embryos and found mutagenesis efficiencies up to 94.7% in the F0 embryos ($n = 36/38$ injected embryos) (Fig. 3*H–J*). To validate the extent of mutagenesis, we cloned 18 individual PCR amplicons each from two F0 embryos. Sanger sequencing showed that all 36 PCR products had mutations (deletions or insertions); 27/36 amplicons were out-of-frame and would cause a stop or an early protein truncation. The remaining nine in-frame mutations caused a variety of short amino acid insertions or deletions.

We injected Tg(*foxP2-enhancerA.2:egfp-caax*) embryos with *htr2ab* CRISPR/Cas9 sgRNA and found that F0-injected embryos had failure of TCPTc commissure formation and a decreased C/L1 ratio (Fig. 3*E*). The TCPTc formation defects induced by CRISPR/Cas9 sgRNA were rescued when coinjected with *htr2ab* mRNA (Fig. 3*E*,*G*), indicating the specificity of CRISPR/Cas9 sgRNA. We validated that the CRISPR was still functional in the coinjected embryos by PCR analysis at the endogenous *htr2ab* locus, indicating that the rescue was due to the *htr2ab* mRNA and was not due to failure of mutagenesis induced by CRISPR/Cas9 sgRNA. Therefore, loss of *htr2ab*, either by morpholino knock-down or CRISPR gene disruption, leads to midline-crossing er-

←

(*Figure legend continued.*) compared with control axon pathways showing that, in treated embryos, the C/L ratio was decreased, indicating fewer TCPTc axons crossing the midline. ***K***, No change was seen in the L2/L1 ratios between control and ketanserin-treated embryos, indicating that the misguided axons did not preferentially choose the longitudinal tract. ***L***, Intensity ratio data shown with values normalized to controls. Error bars indicate SEM. ***M***, C/L1 ratios showing effects of different developmental timing exposure of ketanserin. Effects of ketanserin were developmentally maximal from 48 to 72 hpf, whereas treatment with ketanserin from 72 to 96 hpf did not affect the TCPTc. $*p < 0.05$, $**p < 0.01$; Student's *t test*. Error bars indicate SEM. ***N***, ***O***, Confocal images at 72hpf of sparse labeling in embryos transiently injected with plasmids for *foxP2-enhancerA.2:Gal4* and *UAS:GFP-caax*. ***P***, Quantification of sparse labeling: control embryos ($n = 10$) demonstrate midline crossing that is disrupted by ketanserin ($n = 11$) Error bars indicate SE of the proportion. ***Q***, Normalized quantification of anterior commissure midline axon crossing area and fluorescence intensity of Tg(*foxP2-enhancerA.2:egfp-caax*) embryos shows no affect of ketanserin. Error bars indicate SEM.

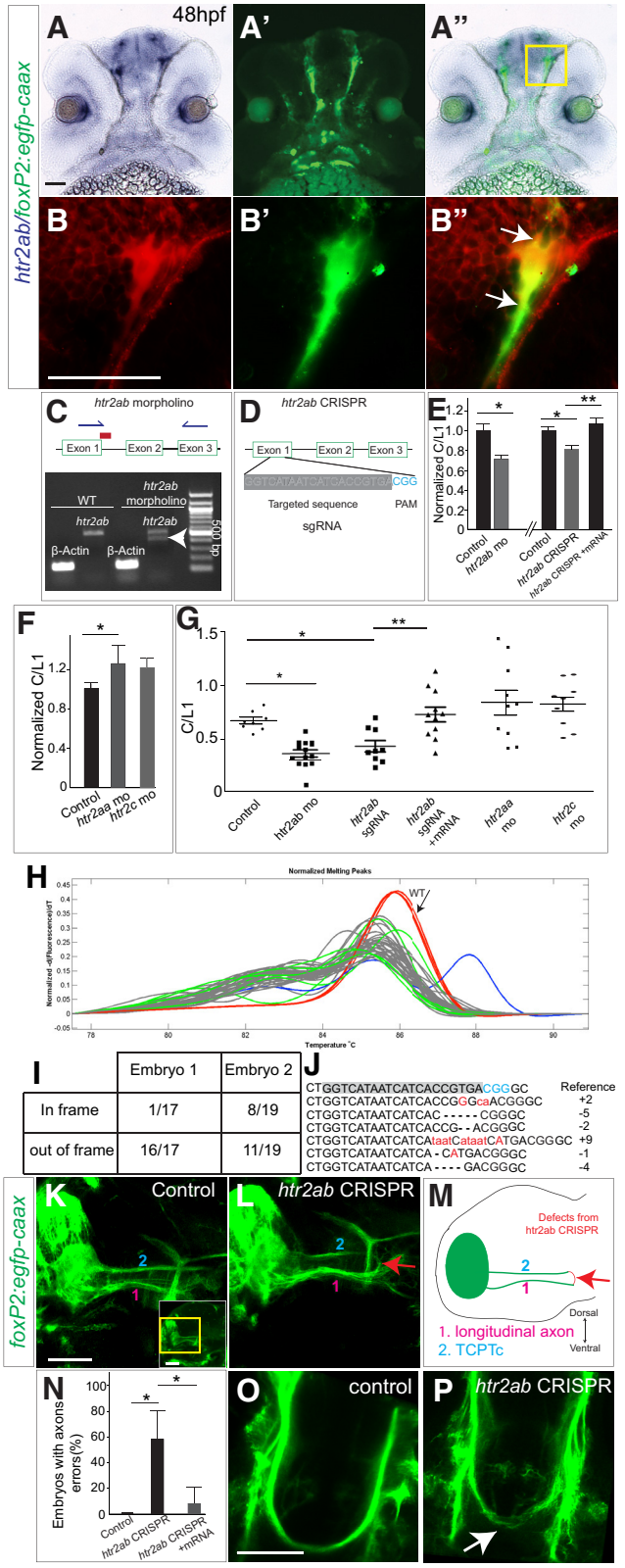

Figure 3. *htr2ab* is necessary for TCPTc formation. ***A–B′′***, Sections of 48hpf Tg(*foxP2-enhancerA.2:egfp-caax*) embryo double-labeled for *htr2ab in situ* and α-GFP, rostral top. Scale bar, 50 μm. Bright-field (***A***), fluorescent (***A′***), and merged images (***A′′***) show *htr2ab* expression in *foxP2* neurons and in axon tracts. ***B–B′′***, Higher magnification of boxed region in ***A′′***. ***C***, *htr2ab* splice-blocking morpholino targets exon 1/intron 1 boundary. Gel shows that morpholino partially blocks normal splicing (arrowhead). ***D***, Schematic of *htr2ab* sgRNA used in CRISPR experiments. ***E***, *htr2ab* knock-down causes decreased TCPTc midline axon crossing. C/L1 normalized ratio data of TCPTc crossing. *htr2ab* morpholino or sgRNA/Cas9-injected embryos have lower C/L1 ratios, indicating failure of midline axon crossing. C/L1 ratio is rescued in embryos coinjected with *htr2ab* mRNA and sgRNA/Cas9. ($n = 11, 14, 10, 9, 11$, respectively in columns). $^{*}p < 0.05$, $^{**}p < 0.01$, Student's *t* test for morpholino; one-way ANOVA with Turkey's *post hoc* test for CRISPR). Error bars indicate SEM. ***F***, Scatterplot of C/L1 ratios shows that morpholino mediated knock-down of *htr2aa* and *htr2ac* does not affect axon pathfinding. ***G***, Normalized C/L1 ratios in *htr2aa* and *htr2c* morpholino-injected embryos. ***H***, HRMA (Xing et al., 2014) of PCR products shows that 36 of 38 embryos injected with *htr2ab* sgRNA/Cas9 have an abnormal melt curve, indicating a mutation. ***I***, Proportion of in-frame and out-of-frame mutations sequenced from *htr2ab* PCR amplicons for two embryos (all PCR products had mutations). ***J***, Sequences from cloned PCR amplicons from *htr2ab* CRISPR. The target site and protospacer adjacent motif (PAM) are highlighted in gray and blue, respectively. Representative sequences of *htr2ab* mutations in the F0 are shown. Insertions, deletions, and point mutations are shown as, respectively, red lower case letters, dashes, and upper case letters. ***K***, ***L***, Lateral views of 48 hpf Tg(*foxP2-enhancerA.2:egfp-caax*) embryos, confocal *z*-stacks. Yellow region of inset indicates region shown in panels. ***M***, Schematic illustration of findings. TCPT axons (2) project caudally before turning medially (not seen in this *z*-stack). Longitudinal axons (1) run parallel but more ventral. In an *htr2ab* CRISPR-injected embryo, TCPT axons erroneously leave (red arrow) the TCPT tract and join the longitudinal axons. Scale bar, 50 μm. ***N***, Quantification of pathfinding errors caused by *htr2ab* CRISPR, which is rescued by coinjection with *htr2ab* mRNA ($^{*}p < 0.05$). ***O***, ***P***, Oblique dorsal views of 72 hpf Tg(*foxP2-enhancerA.2:egfp-caax*) embryos and confocal *z*-stacks shows that htr2ab CRISPR also leads to dorsal–ventral spreading of TCPT commissure (arrow). Scale bar, 50 μm.

rors in the TCPTc, supporting a role for 5-HT signaling in the TCPT axons as they decussate.

Using the *htr2ab* CRISPR, we clarified the route followed by aberrantly projecting TCPTc axons. We viewed the TCPT tracts laterally in CRISPR-injected embryos and found that TCPT axons would aberrantly leave the TCPT and join a longitudinal commissure immediately ventral and parallel to the TCPT tract instead of crossing the midline (Fig. 3*K–N*). Therefore, the misprojected TCPTc axons joined the "L2" tract, thus explaining why the L2/L1 ratio remained unchanged in ketanserin-treated embryos (Fig. 2*K*). In addition, those TCPT axons that still crossed the midline defasciculated in a broader dorsal–ventral bundle (Fig. 3*O*,*P*).

Raphe neuron serotonin expression is necessary for commissure formation

Because our data suggested a role for the *htr2ab* receptor and 5-HT signaling in the midline crossing of TCPTc axons, we next investigated whether a source of 5-HT was available to the TCPTc axon growth cones during development. In zebrafish, the dorsal raphe nucleus expresses 5-HT by 36 hpf and 5-HT axonal projections are widely distributed in the CNS by 72 hpf (Lillesaar et al., 2009). To determine whether TCPTc axons encountered a 5-HT source, we performed immunostaining for 5-HT and for GFP in Tg(*foxP2-enhancerA.2:egfp-caax*) embryos. We found that serotonin-expressing neurons had projections neighboring the ends of TCPTc axons before their midline crossing at 48 hpf (Fig. 4*A*,*A′′*. We confirmed this in confocal, single-slice, high-resolution images (Fig. 4*B*,*B′′*,*C–E*).

In zebrafish, unlike mammals, several 5-HT nuclei are present in the CNS (Kaslin and Panula, 2001; McLean and Fetcho, 2004; Lillesaar, 2011), including pretectal and posterior tuberculum/hypothalamic nuclei (Fig. 4*A′*, arrowhead). To determine whether the raphe nuclei were the source of the serotonergic projections for the TCPTc axons, we used an enhancer for 5-HT neurons specific to the raphe nucleus, −*3.2pet1* (referred to as "*pet1*") (Lillesaar et al., 2009). We examined axon projections from the raphe 5-HT neurons to the TCPTc axons in triple-transgenic animals: Tg(*pet1:Gal4*), Tg(*UAS:RFP-caax*), and Tg(*foxP2-enhancerA.2:egfp-caax*). We observed RFP-expressing

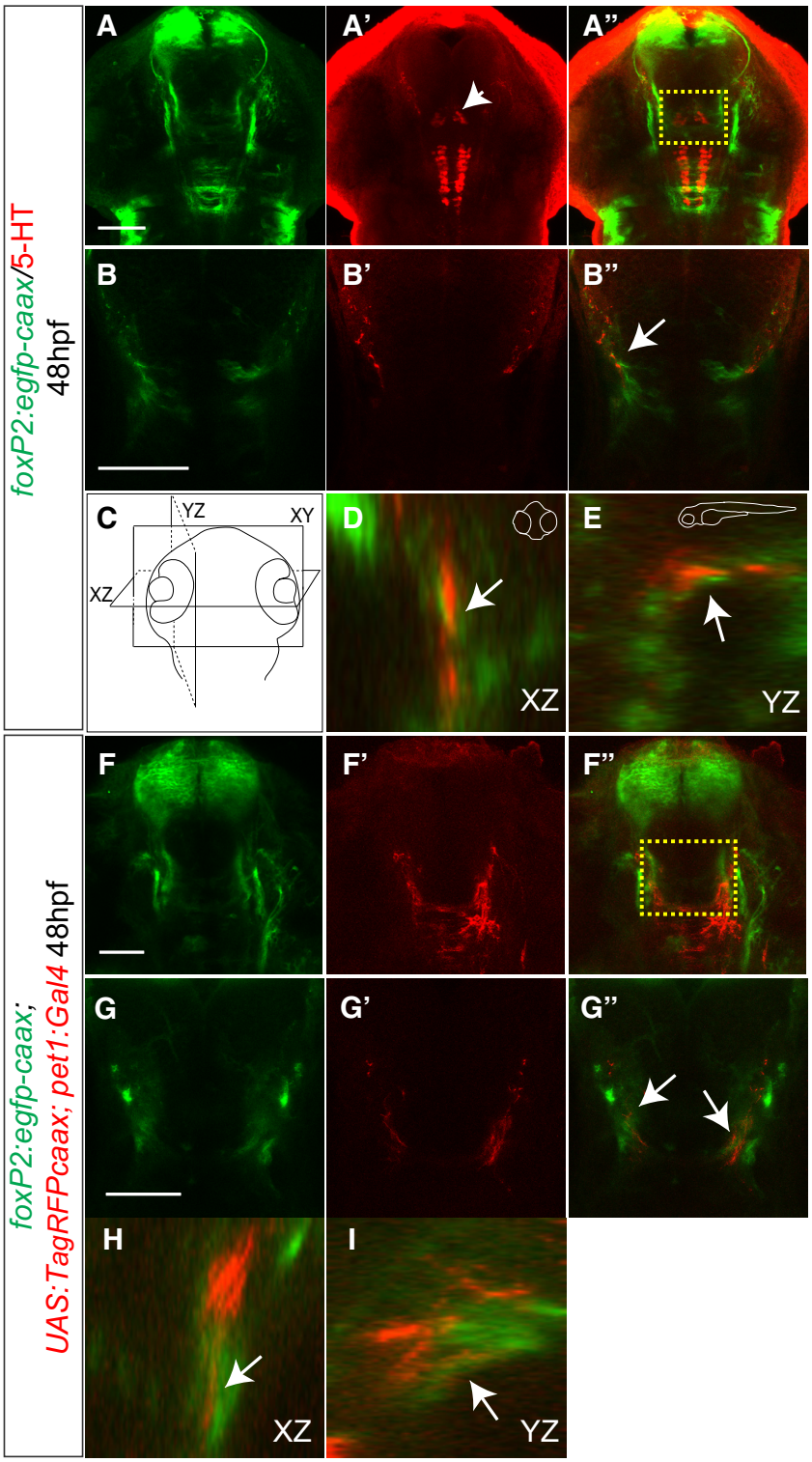

Figure 4. Serotonergic neurons project in close apposition to TCPTc commissural axon tips before midline crossing. ***A–B′′***, Confocal images of whole-mount embryo at 48 hpf, rostral top. Scale bar 50 μm. Tg(*foxP2-enhancerA.2:egfp-caax*) embryo double-labeled for α-GFP and for α-5-HT. Boxed region in ***A′′*** is shown at higher resolution in ***B–B′′*** as a single confocal slice. Arrow points to serotonin-expressing axon projections (red) overlapping *foxP2* TCPTc developing axons (green). ***C–E***, XZ and YZ plane projections from consecutive confocal slices confirm the overlap between 5-HT axons and TCPTc growth cones. ***F–G′′***, Confocal images of Tg(*foxP2-enhancerA.2:egfp-caax*), Tg(*pet1:Gal4*), and Tg(*UAS:RFP-caax*) whole-mount embryos at 56 hpf, rostral top. Scale bar, 50 μm. Shown is double immunohistochemistry for α-GFP and α-RFP demonstrating that the raphe nucleus axons could provide 5-HT for *foxP2* axons. Boxed region in ***F′′*** is shown in higher resolution in ***G–G′′*** as a single confocal slice. Arrows in ***G*** point to RFP expression from raphe nuclei overlapping TCPTc growth cone. ***H***, ***I***, XZ and YZ plane projections from consecutive confocal slices confirm the overlap between RFP-expressing axons and TCPTc growth cones.

axons from the raphe nuclei projecting to the TCPTc axons (Fig. 4*F–I*), including in single slice confocal images, confirming that the raphe neurons are the likely source of 5-HT for TCPTc axons.

To determine whether the raphe neurons are necessary to provide 5-HT for TCPTc midline crossing, we performed targeted genetic ablation of the raphe. We used the cell-autonomous nitroreductase/metronidazole system (Curado et al., 2008; Pisharath and Parsons, 2009), driving expression of nitroreductase [Tg(*UAS:NTR-mCherry*)] in raphe 5-HT neurons using Tg(*tph2:Gal4*) (Yokogawa et al., 2012), and visualized expression of axons with *Tg(foxP2-enhancerA.2:egfp-caax*) (Fig. 5*A*). We used the Tg(*tph2:Gal4*) line because we noted that Tg(*pet1:Gal4*) expressed in fewer 5-HT raphe neurons. In the absence of metronidazole, there was no ablation of raphe neurons and TCPTc axon pathfinding was normal (Fig. 5*B*,*D*,*F*). With the addition of metronidazole, ablation of raphe neurons occurred in embryos expressing nitroreductase, with loss of 5-HT and disruption of TCPTc midline crossing (Fig. 5*C*,*E*,*G*). In embryos with no nitroreductase, metronidazole had no significant effect on midline axon crossing or on the number of 5-HT neurons (Fig. 5*H*,*I*). Metronidazole treatment and ablation of raphe neurons did not cause nonspecific apoptosis of other neuron groups in the region of the TCPTc or disruption of other diencephalic midline crossing (Fig. 5*J–M*). These results show that 5-HT is necessary for TCPTc midline crossing and demonstrate that the raphe nucleus is the likely source of 5-HT.

ephrinB2a limits midline crossing and mediates 5-HT action on pathfinding

We had shown previously that the transmembrane ligand *ephrinB2a* is involved in TCPTc axon midline crossing and that its ligand *ephA4a* is expressed in a complementary pattern to the TCPT axons in the CNS midline (Stevenson et al., 2012). The *ephrinB* family of ligands are known to be involved in midline commissure formation (Imondi and Kaprielian, 2001; Kadison et al., 2006). To determine whether 5-HT's role in TCPTc midline axon guidance could be mediated by ephrinB2a, we obtained and characterized an *ephrinB2a* mutant allele, $efnB2a^{hu3393}$, from the Zebrafish Mutation Project (Wellcome Trust Sanger Institute; Kettleborough et al., 2013). $efnB2a^{hu3393}$ is a nonsense mutation in exon 2 of *ephrinB2a* (T>A; C86X) (Fig. 6*A*). $efnB2a^{hu3393}$

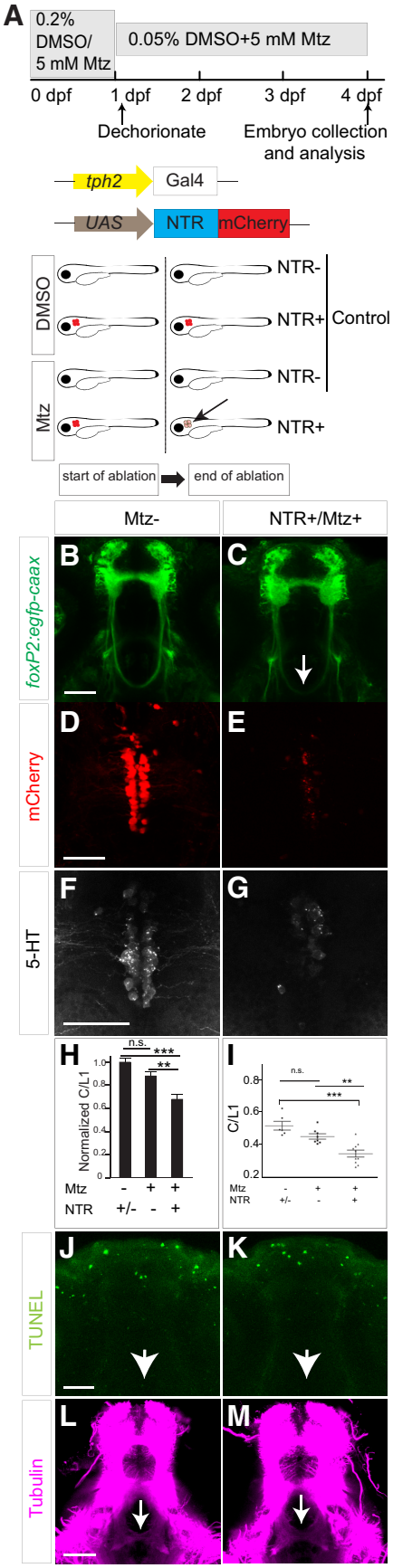

Figure 5. Ablation of the 5-HT neurons causes TCPTc midline-crossing defects. ***A***, Schematic diagram of nitroreductase (NTR)/Mtz experiments. Shown are *tph2:Gal4* embryos treated with Mtz from 0 to 96 hpf. In double-transgenic animals (*tph2:Gal4*; *UAS:NTR-mCherry*), Mtz is converted to a toxic metabolite, causing apoptosis of 5-HT/*tph2* neurons. ***B–G***, Confocal images of a whole-mount embryo at 96 hpf, rostral top. Scale bar, 50 μm. ***B***, Embryos without Mtz treatment. ***C***, Mtz treatment leads to axon-crossing defects in embryos expressing *tph2:Gal4/UAS:NTR-mCherry*. ***D***, ***F***, Embryos without Mtz treatment, immunohistochemistry for mCherry (***D***), or 5-HT (***F***). ***E***, ***G***, Embryos expressing *tph2:Gal4/UAS:NTR-mCherry* treated with Mtz, immunohistochemistry for mCherry (***E***) or 5-HT (***G***). ***H***, Normalized C/L1 ratios show that ablation of raphe nuclei leads to the failure of TCPTc axon crossing. $n = 6$, 8, and 10, respectively, in columns. $^{**}p < 0.01$, $^{***}p < 0.001$, one-way ANOVA with Turkey's *post hoc* test. n.s., Not significant. Error bars indicate SEM. ***I***, Scatterplot C/L1 values of data shown in ***H***. ***J***, ***K***, TUNEL staining in control and Mtz-treated animals shows no evidence of increased apoptosis in region of TCPTc (arrows). ***L***, ***M***, Midline crossing of other axon tracts in the diencephalon is not perturbed by raphe neuron ablation and Mtz treatment. Confocal *z*-stack images of 72 hpf embryos, rostral top, staining for anti-acetylated tubulin. Scale bar, 50 μm.

homozygotes (*efnB2a*$^{-/-}$) are viable and immunohistochemistry demonstrates loss of ephrinB2a protein (Fig. 6*B*,*C*). Tubulin staining of homozygous mutants did not show gross defects in major axon tracts (Fig. 6*D–G*). The TCPTc commissure appeared normal on visual inspection in the homozygous *efnB2a*$^{-/-}$ background (Fig. 6*J*), but there was a statistically significant increase in the number of crossing axons (Fig. 6*L*,*N*).

Blockade of 5-HT signaling in *efnB2a*$^{+/-}$ heterozygotes by ketanserin causes TCPTc axon pathfinding defects similar to that seen in a wild-type background (Fig. 6*H*,*I*,*L*,*N*). However, in *efnB2a*$^{-/-}$ homozygous mutants treated with ketanserin, TCPTc midline axon crossing was normal (Fig. 6*J–L*,*N*). *efnB2a*$^{-/-}$ mutants do not have a change in raphe 5-HT expression (Fig. 6*M*,*M*′). These results show a role for ephrinB2a in normally limiting midline axon crossing and in mediating the action of 5-HT on the TCPTc decussation.

5-HT regulates ephrinB2a translation in the axon

How does 5-HT signaling interact with *ephrinB2a* regulation of TCPTc midline axon crossing? Axon guidance molecule expression can be regulated or modified by transcription, translation, or posttranslational processes (Winckler and Mellman, 2010; Jung et al., 2011; Hancock et al., 2014). 5-HT has the capability to stimulate translation in subcellular domains of target cells (Martin et al., 1997; Casadio et al., 1999; Miniaci et al., 2008), a possible mechanism by which it could regulate axon guidance receptor activity.

To address these potential mechanisms, we examined levels of *ephrinB2a* in ketanserin-treated embryos. We found no significant difference in overall *ephrinB2a* RNA transcript levels by RT-PCR in whole embryos. However, after ketanserin treatment, we noted increased ephrinB2a protein levels in embryos by quantification of immunofluorescence levels, including in the telencephalon and TCPTc axons (Fig. 7*A–C*), but not in the eyes. This was also confirmed by Western blot quantification of whole-embryo extracts (Fig. 7*C*). To demonstrate that ketanserin's effect on ephrinB2a levels was dependent on 5-HT, we performed ablation of raphe 5-HT neurons in Tg(*tph2:Gal4*); Tg(*UAS:NTR-mCherry*) embryos. We found that raphe neuron ablation led to an increase of ephrinB2a protein levels in the TCPTc axons, but not in the telencephalon and eyes (Fig. 7*D–G*).

5-HT responds to hypoxia to decrease midline axon crossing

Because 5-HT has demonstrated roles in mediating adult plasticity, we considered whether 5-HT might also have a role in regulating axon guidance in response to environmental or developmental factors. Interpretation of external factors and changes to developing circuitry would be a mechanism by

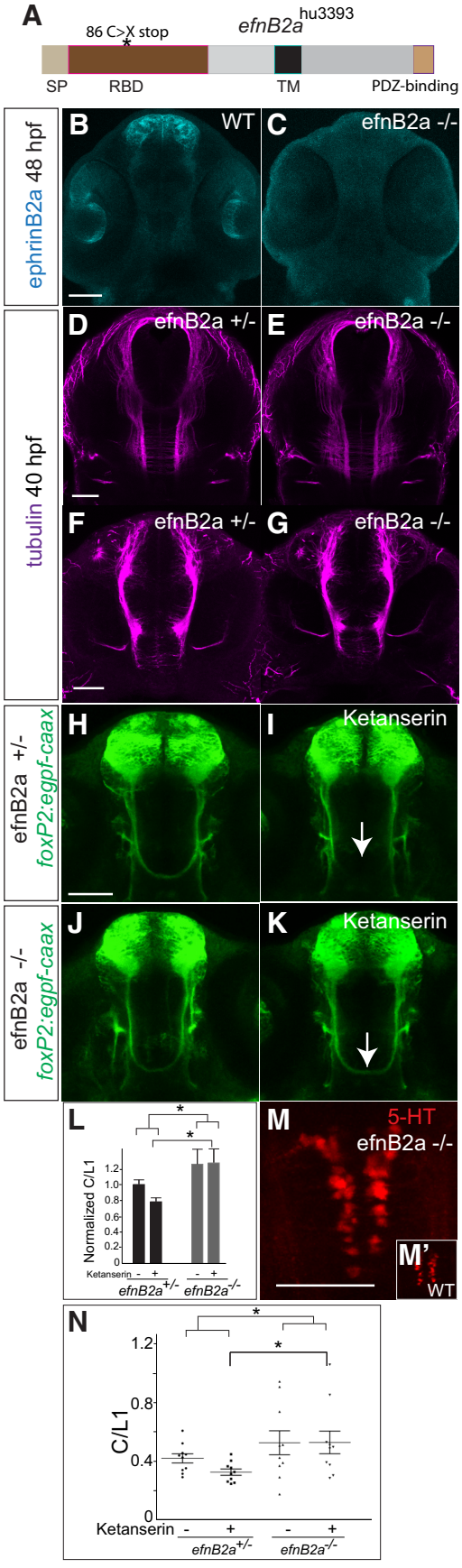

Figure 6. 5-HT mediates axon guidance through *ephrinB2a* (*efnB2a*). ***A***, The *efnB2a* ^{hu3393} allele is a nonsense mutation in the receptor-binding domain (exon 2) of *ephrinB2a* (T>A; C86X). SP, Signal peptide; RBD, receptor-binding domain; TM, transmembrane domain. ***B–K***, ***M***, ***M′***, Confocal images, rostral top. Scale bar, 50 μm. ***B***, ***C***, efnB2 immunohistochemistry. efnB2 protein is absent in the *efnB2a* $^{hu3393/hu3393}$ (*efnB2a* $^{-/-}$) embryo compared with WT. ***D–G***, Acetylated tubulin immunohistochemistry does not show gross axon defects in *efnB2a* $^{-/-}$ embryos. ***D***, ***E***, Axons in dorsal brain. ***F***, ***G***, Axons in ventral brain. ***H–K***, GFP immunohistochemistry in Tg(*foxP2-enhancerA.2:egfp-caax*) embryos shows that lack of efnB2 (in *efnB2a* $^{-/-}$ embryos; ***J***, ***K***) prevents ketanserin-induced midline crossing defects (arrow) compared with *efnB2a* heterozygotes (***H***, ***I***). ***L***, Quantification confirms that *efnB2a* $^{-/-}$ restores axon guidance in presence of ketanserin. $n = 10$ per group. *$p < 0.05$, two-way ANOVA followed by Bonferroni post test. Error bars indicate SEM. ***M***, *efnB2a* $^{-/-}$ mutant has normal raphe 5-HT expression compared with WT (***M′***). ***N***, Scatterplot of C/L1 raw data results for ***L***.

which a developing organism could modify its regulation of connectivity. Our previous work demonstrated that hypoxia disrupts midline axon crossing by increasing levels of ephrinB2a (Stevenson et al., 2012). In nematodes, hypoxia increases 5-HT expression with a resultant activation of a latent sensory circuit (Pocock and Hobert, 2010). To determine whether hypoxia affects 5-HT expression, we exposed developing zebrafish embryos to hypoxia from 24 to 36 hpf (Stevenson et al., 2012) and examined levels of 5-HT at 72 hpf. We found a decrease in 5-HT levels at 72 hpf (Fig. 8*A–D*), but normal cell counts in the raphe. Measurement of 5-HT via HPLC showed a significant decrease in embryo 5-HT levels from 1.0 to 0.8 pg/μg in hypoxia ($n = 100$ embryos each; SEM 0.02, $p < 0.001$; Fig. 8*N*). Hypoxia's effect on 5-HT expression was specific because there were no effects on apoptosis or general embryo viability (Stevenson et al., 2012) and because levels of expression of the pan-neuronal marker Elav family members anti-HuC/D were unaffected (Fig. 8*C*,*D*).

Tryptophan hydroxylase (*tph*) is the rate-limiting enzyme for 5-HT biosynthesis; raphe neurons in zebrafish express the Tph ortholog *tph2* (Bellipanni et al., 2002; Teraoka et al., 2004). *tph* expression in other species has been shown to be responsive to hypoxia (Rahman and Thomas, 2009; Pocock and Hobert, 2010). Using qRT-PCR, we found that, after hypoxia, *tph2* RNA expression was decreased in the raphe nucleus. The decrease in *tph2* was present at 36 hpf immediately after cessation of hypoxia and persisted at 48 hpf (Fig. 8*E*,*F*).

Because hypoxia decreased 5-HT levels, we reasoned that rescuing 5-HT signaling in hypoxia embryos should prevent midline axon-crossing errors. To test this, we incubated hypoxic embryos with fluoxetine, a selective 5-HT reuptake inhibitor that increases available 5-HT at the synapse. We found that fluoxetine incubation from 24 to 72 hpf rescued the effect of hypoxia on midline axon crossing (Fig. 8*G–J*). Interestingly, incubation of embryos with fluoxetine starting at 24 hpf increased the axon crossing by 52 hpf (Fig. 8*K*,*L*), further supporting that a balance of 5-HT signaling is important for midline crossing. To determine whether fluoxetine acted by affecting ephrinB2a levels, we measured levels of ephrinB2a levels in the TCPTc axons as they crossed the midline at 36 hpf. We found that fluoxetine decreased ephrinB2a levels in the crossing TCPT axons under both control and hypoxia conditions (Fig. 8*M*). Hypoxia did not affect the overall distribution of raphe 5-HT axon projections. These data show that raphe neurons can respond to environmental hypoxia and modulate 5-HT expression, thereby altering neural circuit development.

Discussion

We have found that 5-HT and its receptor, *htr2ab*, provide instructive guidance for midline axon crossing through downregulation of ephrinB2a levels. 5-HT's role is sensitive to environmental cues because developmental hypoxia decreases 5-HT expression from the

←

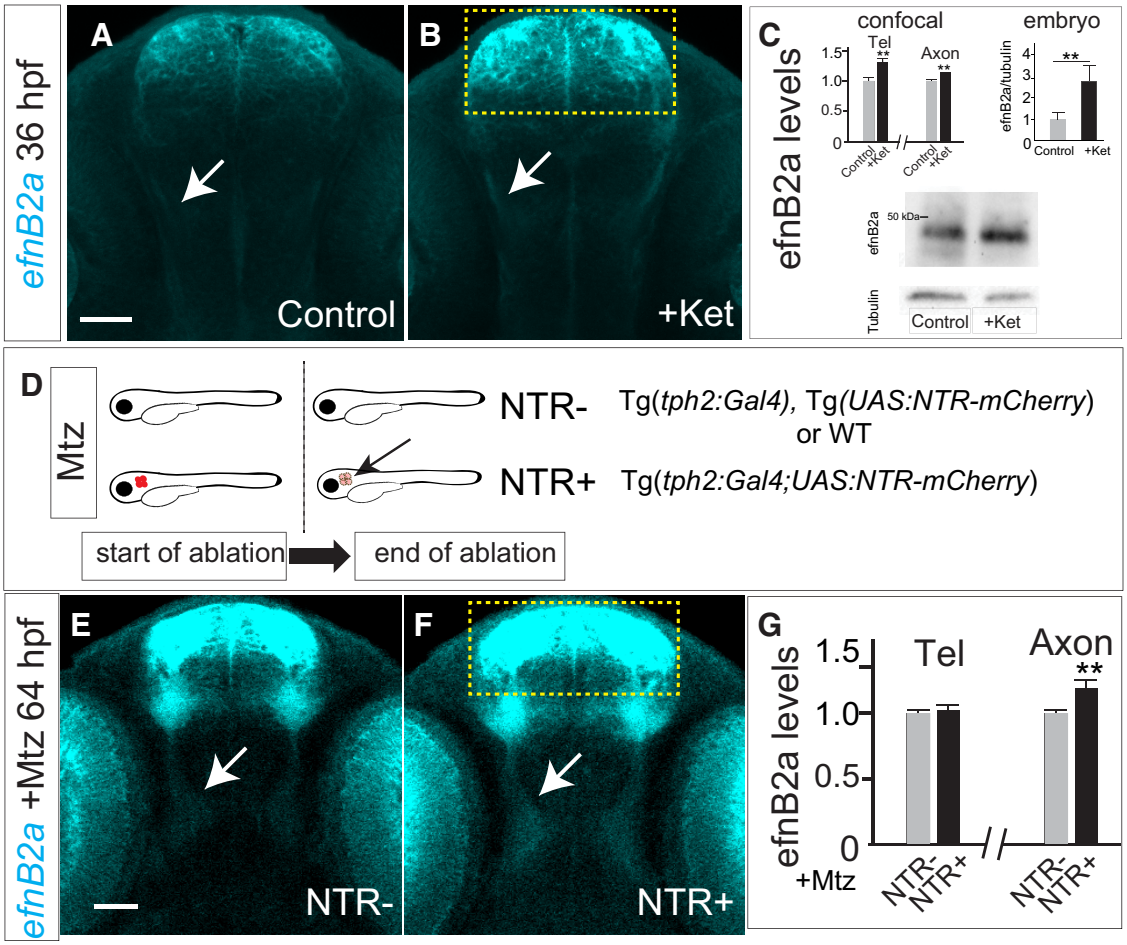

Figure 7. 5-HT regulates efnB2a protein levels. ***A***, ***B***, ***E***, ***F***, Confocal images, 36hpf embryos, immunohistochemistry for α-efnB2a, rostral top. Scale bar, 50 μm. ***A***, ***B***, efnB2a levels are increased in telencephalon (boxed region) and TCPTc axons (arrows) in embryos treated with ketanserin (***B***) compared with control (***A***). ***C***, Quantification shows that ketanserin reduces efnB2a levels. Bar graphs show confocal (left) and whole embryo (right) quantification: in telencephalon and TCPTc axons ($n = 20, 14$, respectively, in control and embryos treated with ketanserin. $^{**}p < 0.01$, Student's *t* test. Error bars indicate SEM. Shown are Western blotting bar graph quantification and blots (triplicate). $n = 5$ embryos each experiment; $^{**}p < 0.01$, Mann–Whitney test. Error bars indicate SEM. ***D***, Schematic illustration of Mtz treatment in NTR$^-$ and NTR$^+$ embryos. Genotypes in each group are shown on right. Note that ablation can occur only when both *tph2:Gal4* and *UAS:NTR-mCherry* are expressed. ***E***, ***F***, efnB2a levels in TCPTc axons (arrows) are increased, but not in the telencephalon (boxed region), in embryos expressing *tph2:Gal4/UAS:NTR-mCherry* (***F***) compared with embryos without *NTR* expression (***E***) after treatment with Mtz. ***G***, Quantification of efnB2a levels in telencephalon and TCPTc axons. $n = 10, 12$, respectively, in NTR$^-$ and NTR$^+$ embryos. $^{**}p < 0.01$, Student's *t* test.

raphe neurons and causes midline-crossing defects. Our findings suggest that modification of the serotonergic system by early environmental exposures may contribute to permanent CNS connectivity alterations.

5-HT and *htr2ab* are necessary for axon guidance

The components of 5-HT signaling are conserved over 2 billion years of evolution from protozoa to mammals (Azmitia, 2007). During evolution, 5-HT's roles and localization of action have become increasingly more specialized. In unicellular eukaryotes such as the ciliate protozoa *Tetrahymena*, 5-HT acts in intracellular signaling; in primitive metazoans such as *Planaria*, 5-HT has additional roles in hormonal cell–cell signaling; and in the nervous system of arthropods and vertebrates, 5-HT acts as a neurotransmitter at synapses (Turlejski, 1996; Hay-Schmidt, 2000). In mammals, 5-HT signaling plays important roles in regulating behavior, memory consolidation, sleep, and appetite (Gingrich et al., 2003). Abnormalities in the 5-HT system in humans are associated with a range of neurobehavioral and neuropsychiatric disorders (Lesch and Waider, 2012; Blasi et al., 2013; Harrington et al., 2013).

Roles for 5-HT in early CNS development have recently been uncovered, including in neuron migration, dendrite arborization, and synapse formation (Persico et al., 2001; Matsukawa et al., 2003; Vitalis et al., 2007; Riccio et al., 2009). 5-HT signaling has been suggested to regulate axon guidance: in mice, overexpression of 5-HT receptors causes a shift in thalamocortical axon tracts (Bonnin et al., 2007) and rats lacking the 5-HT transporter had altered raphe-prefrontal cortex pathways (Witteveen et al., 2013). We found that 5-HT, acting through *htr2ab*, an excitatory G-protein-coupled receptor (GPCR), is necessary for normal midline axon crossing. We confirmed this finding using pharmacological blockade of *htr2*, as well as with both morpholino and CRISPR/Cas9 knock-down of *htr2ab*. We found that the source of the 5-HT is from neurons of the raphe nucleus, by demonstrating close apposition of 5-HT axon termini to the termini of TCPTc axons. Further, using cell-type-specific genetic ablation, we demonstrated that raphe neurons are a necessary source of 5-HT TCPT axon development. However, we cannot fully exclude the involvement of other 5-HT sources as well; for example, the cell cluster located medially and anterior to the paraventricular organ (Lillesaar et al., 2009). Other *htr2* receptors in addition

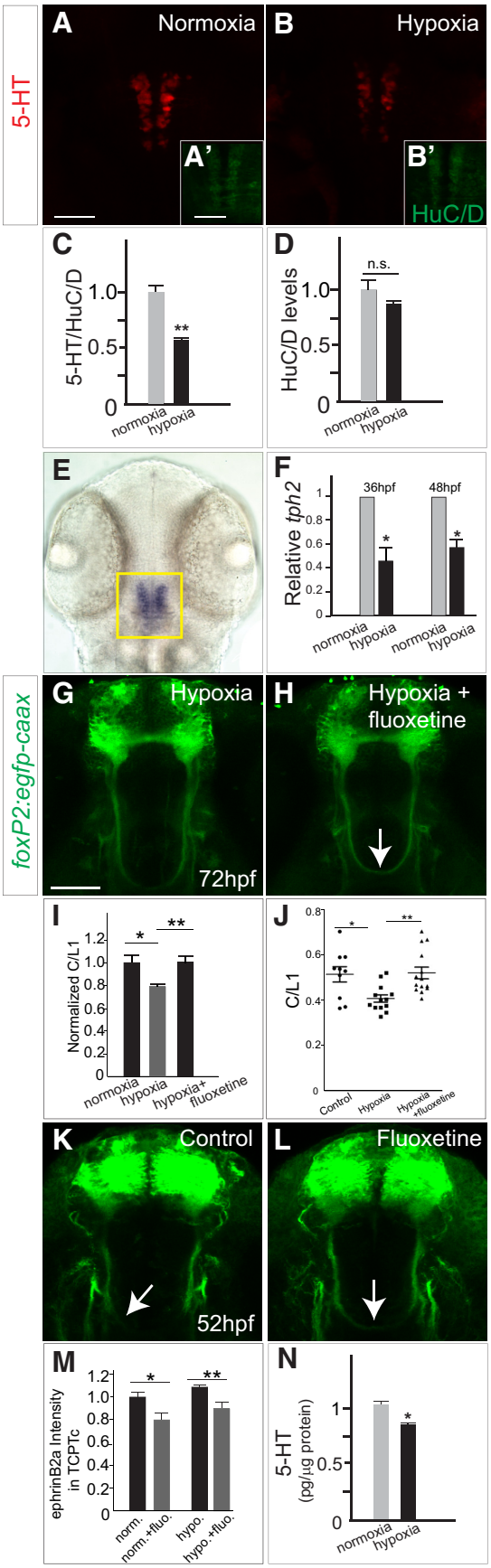

Figure 8. 5-HT signaling is an interpreter of developmental environment to control TCPTc midline crossing. ***A–B′***, Hypoxia decreases 5-HT expression. Shown is normoxia compared with hypoxia in confocal images of WT embryos at 48 hpf, maximal intensity *z*-stack projections, stained with 5-HT (***A***, ***B***), stained with HuC/D (***A′***, ***B′***), rostral top. Scale bar, 50 μm. ***C***, 5-HT levels in raphe neurons (normalized to pan-neuronal marker HuC/D) are significantly decreased by hypoxia. $n = 6$ per group, $^{**}p < 0.01$ Student's *t* test. ***D***, HuC/D levels are not changed after hypoxia. $n = 6$ per group. Error bars indicate SEM. ***E***, Bright-field *in situ* image showing that *tph2* mRNA is specifically expressed in raphe. ***F***, *tph2* mRNA levels (qRT-PCR) are decreased in 36 and 48 hpf posthypoxic embryos. Error bars indicate SEM (three experimental replicates). ***G***, ***H***, Confocal images of Tg(*foxP2-enhancerA.2:egfp-caax*) show that fluoxetine (***H***) rescues axon guidance defects in hypoxic embryos (***G***) at 72 hpf. ***I***, ***J***, Normalized (***I***) and scatterplot raw (***J***) C/L1 ratio data confirms fluoxetine rescue of hypoxia effects. $n = 10, 13, 14$, respectively, in columns. $^{*}p < 0.05$, $^{**}p < 0.01$, one-way ANOVA followed by Turkey's *post hoc* test. Error bars indicate SEM. ***K***, ***L***, confocal images of Tg(*foxP2-enhancerA.2:egfp-caax*) show that fluoxetine (***L***) increases the number of axons crossing the midline by 52 hpf. ***M***, Quantification of ephrinB2a protein levels in TCPTc axons at 36 hpf shows that fluoxetine decreases ephrinB2a levels under both control (normoxic) and hypoxic conditions. $n = 5, 4, 5, 4$ embryos, respectively. $^{*}p < 0.05$, $^{**}p < 0.01$, Student's *t* test. Error bars indicate SEM. ***N***, HPLC-ED demonstrates a significant decrease in embryo 5-HT levels from 1.0 to 0.8 pg/μg in hypoxia. $n = 100$ embryos each; SEM = 0.02. $p < 0.001$, Student's *t* test.

to *htr2ab* may be necessary for the guidance, but we could not test this because of whole embryo early lethality when we knocked down several receptors simultaneously. Further, additional levels of complexity may exist with respect to control of TCPTc midline crossing because different TCPT commissural axons may express different receptors affecting crossing.

Our experiments do not specifically address whether 5-HT affects the guidance of other axon tracts; for example, differentiating whether 5-HT preferentially affects midline versus longitudinal tracts. Because the TCPT commissure has relatively fewer axons than larger tracts such as the anterior commissure, we were able to detect errors made by a smaller number of axons. It is also unclear whether 5-HT acts solely through effects on ephrinB2a or if it also affects other guidance molecule expression or mechanisms of action. We have noted that *netrin1a* levels are not affected by ketanserin in the embryo (data not shown), but 5-HT could still act by different mechanisms. For example, in the mouse, 5-HT changes netrin-1 signaling from an attractive to a repulsive cue (Bonnin et al., 2007).

ephrinB2a mediates serotonin-associated axon pathfinding

ephrinB2 acts as a ligand for receptor tyrosine kinases (RTKs) of the EphA and EphB families, inducing an intracellular signaling cascade in the RTK-expressing cell (Bashaw and Klein, 2010). EphrinB ligands are also known to "reverse" signal (Pasquale, 2008; Taylor et al., 2012), which we observed in previous studies on TCPTc pathfinding in the setting of hypoxia (Stevenson et al., 2012). Several studies have demonstrated that ephrinB signaling can function in midline crossing. For example, in *Xenopus*, ephrinB regulates ipsilateral sorting of retinal axons at the midline optic chiasm (Nakagawa et al., 2000); in chick, ephB2 expression at the midline repels axons at older ages (Cramer et al., 2006).

We found that pharmacological blockade of serotonergic signaling through its GPCR, *htr2a*, or ablation of the raphe 5-HT neurons increased ephrinB2a protein levels in the TCPTc axons. This increase in ephrinB2a could be due to increased transcription: both GPCRs and transcription factors, including *Tbx5* and *VAX2*, have been shown to alter ephrinB transcription levels (Jassen et al., 2006; Polleux et al., 2007). However, when we measured *ephrinB2a* mRNA levels using qRT-PCR, we did not observe changes in embryos treated with an *htr2a* antagonist; however, we cannot exclude the possibility that local or subtle changes in *ephrinB2a* transcript levels are masked. Therefore, our data support a role for 5-HT regulation of ephrinB2a protein levels. This could be by

increased translation of ephrinB2a or by regulation of stability of ephrinB2a. Studies in *Aplysia* neuron cultures show that 5-HT can stimulate translation in subcellular domains of target cells (Martin et al., 1997; Casadio et al., 1999; Miniaci et al., 2008). This effect on translation could be through second messenger systems such as CPEB or CREB as in *Aplysia* or, alternatively, 5-HT might exert its effect through miRNAs. *ephrinB2* can be regulated by multiple miRNAs (Wang et al., 2012) and drugs modifying the serotonergic system can alter miRNA expression (Baudry et al., 2010). miRNAs are present in axon growth cones and can alter local translation (Kaplan et al., 2013). Future studies could examine the interaction between serotonin signaling during development and effects on local translation and axon guidance.

Role of the raphe nucleus and serotonin in embryonic development

We observed that hypoxia disrupts axon connectivity by decreasing 5-HT synthesis. If serotonergic signaling is increased by blockade of 5-HT reuptake, then the effects of hypoxia on TCPTc midline crossing are prevented. Therefore, the raphe nucleus, through regulation of 5-HT levels, which in turn affect midline axon guidance, effectively acts as a sensor to changes in the embryonic milieu. Interestingly, in the adult rat, dorsal raphe 5-HT neurons also respond to the environment, acting as chemoreceptors to changes in blood pH/CO_2 levels with altered firing patterns (Severson et al., 2003).

5-HT axon projections are widespread in early development during the period when extensive axon pathfinding occurs (Rubenstein, 1998; Lillesaar et al., 2009); exposures to serotonergic drugs during gestation have been linked with increased risks for neurodevelopmental disorders (Rai et al., 2013; El Marroun et al., 2014; Gidaya et al., 2014; Harrington et al., 2013) and polymorphisms in genes in the 5-HT signaling pathway are associated with a range of neuropsychiatric disorders (Sutcliffe et al., 2005; Prasad et al., 2009; Kuzelova et al., 2010). Loss or knock-out in early development of 5-HT neurons or other components of 5-HT signaling leads to diffuse CNS abnormalities with a wide range of behavioral phenotypes (Daubert and Condron, 2010; van Kleef et al., 2012). In the invertebrate *C. elegans*, hypoxia can increase 5-HT expression and change a neural circuit response to gustatory sensation (Pocock and Hobert, 2010), providing evidence of biological relevance for an interaction between 5-HT signaling and neural circuits. These lines of evidence, in addition to the work presented here, are consistent with 5-HT acting to mediate changes in how connectivity develops. Future studies can examine the evolutionary and neurobiology significance of 5-HT's role for axon guidance and its responsiveness to external conditions during development.

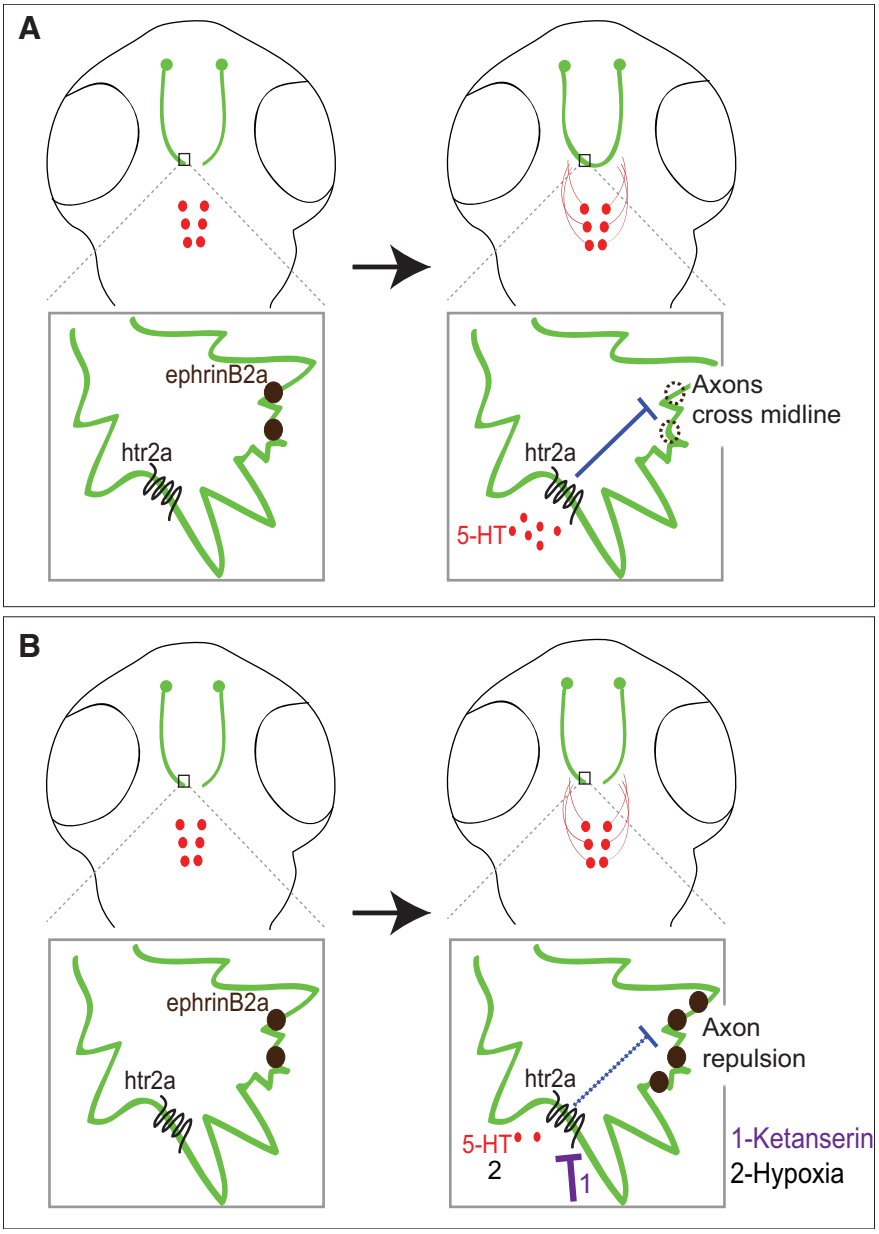

Figure 9. Model. ***A***, During development, TCPTc growth cones are exposed to 5-HT from raphe nuclei axon projections. 5-HT activates htr2ab in the TCPTc, decreasing expression of ephrinB2a and allowing axons to cross the midline. ***B***, When 5-HT signaling is inhibited by drug, knock-down, or hypoxia, the up-regulation of ephrinB2a expression prevents TCPTc axons crossing the midline.

Conclusions

The findings here suggest a model in which serotonergic signaling, supplied by embryonic axon projections from the raphe nucleus, is necessary for normal midline axon crossing (Fig. 9). Our data show a novel link between embryonic environment and early circuit formation, which appears to be mediated in part by an instructive role of 5-HT. Our findings suggest that modification of the serotonergic system during early development can contribute to permanent CNS connectivity alterations. In the presence of 5-HT, levels of ephrinB2a are decreased and axons are able to cross the midline. If 5-HT levels are increased, then axons cross the midline earlier than normal. Conversely, if 5-HT levels

are decreased, such as by pharmacological manipulation or hypoxic exposure, ephrinB2a levels are higher (our data and Stevenson et al., 2012) and axons fail to cross the midline or take abnormal paths. Regulation of midline crossing is complex and includes interacting attractive and repulsive signaling (Evans and Bashaw, 2010). Recent work suggests the possibility for unexpectedly more complex systems of axon guidance, including balancing neuronal activity, although it is not clear whether this applies to midline crossing (Suarez et al., 2014).

References

Azmitia EC (2007) Serotonin and brain: evolution, neuroplasticity, and homeostasis. Int Rev Neurobiol 77:31–56. CrossRef Medline

Barnes NM, Sharp T (1999) A review of central 5-HT receptors and their function. Neuropharmacology 38:1083–1152. CrossRef Medline

Bashaw GJ, Klein R (2010) Signaling from axon guidance receptors. Cold Spring Harb Perspect Biol 2:a001941. Medline

Baudry A, Mouillet-Richard S, Schneider B, Launay JM, Kellermann O (2010) miR-16 targets the serotonin transporter: a new facet for adaptive responses to antidepressants. Science 329:1537–1541. CrossRef Medline

Bellipanni G, Rink E, Bally-Cuif L (2002) Cloning of two tryptophan hydroxylase genes expressed in the diencephalon of the developing zebrafish brain. Mech Dev 119:S215–S220. CrossRef Medline

Blasi G, De Virgilio C, Papazacharias A, Taurisano P, Gelao B, Fazio L, Ursini G, Sinibaldi L, Andriola I, Masellis R, Romano R, Rampino A, Di Giorgio A, Lo Bianco L, Caforio G, Piva F, Popolizio T, Bellantuono C, Todarello O, Kleinman JE, Gadaleta G, Weinberger DR, Bertolino A (2013) Converging evidence for the association of functional genetic variation in the serotonin receptor 2a gene with prefrontal function and olanzapine treatment. JAMA Psychiatry 70:921–930. CrossRef Medline

Bonkowsky JL, Chien CB (2005) Molecular cloning and developmental expression of foxP2 in zebrafish. Dev Dyn 234:740–746. CrossRef Medline

Bonkowsky JL, Wang X, Fujimoto E, Lee JE, Chien CB, Dorsky RI (2008) Domain-specific regulation of foxP2 CNS expression by lef1. BMC Dev Biol 8:103. CrossRef Medline

Bonnin A, Torii M, Wang L, Rakic P, Levitt P (2007) Serotonin modulates the response of embryonic thalamocortical axons to netrin-1. Nat Neurosci 10:588–597. CrossRef Medline

Brogden RN, Sorkin EM (1990) Ketanserin: a review of its pharmacodynamic and pharmacokinetic properties, and therapeutic potential in hypertension and peripheral vascular disease. Drugs 40:903–949. CrossRef Medline

Casadio A, Martin KC, Giustetto M, Zhu H, Chen M, Bartsch D, Bailey CH, Kandel ER (1999) A transient, neuron-wide form of CREB-mediated long-term facilitation can be stabilized at specific synapses by local protein synthesis. Cell 99:221–237. CrossRef Medline

Celada P, Puig MV, Artigas F (2013) Serotonin modulation of cortical neurons and networks. Front Integr Neurosci 7:25. Medline

Choi YB, Li HL, Kassabov SR, Jin I, Puthanveettil SV, Karl KA, Lu Y, Kim JH, Bailey CH, Kandel ER (2011) Neurexin-neuroligin transsynaptic interaction mediates learning-related synaptic remodeling and long-term facilitation in *Aplysia*. Neuron 70:468–481. CrossRef Medline

Cramer KS, Cerretti DP, Siddiqui SA (2006) EphB2 regulates axonal growth at the midline in the developing auditory brainstem. Dev Biol 295:76–89. CrossRef Medline

Curado S, Stainier DY, Anderson RM (2008) Nitroreductase-mediated cell/tissue ablation in zebrafish: a spatially and temporally controlled ablation method with applications in developmental and regeneration studies. Nat Protoc 3:948–954. CrossRef Medline

Dahlström A, Fuxe K (1964) Localization of monoamines in the lower brain stem. Experientia 20:398–399. CrossRef Medline

Daubert EA, Condron BG (2010) Serotonin: a regulator of neuronal morphology and circuitry. Trends Neurosci 33:424–434. CrossRef Medline

Davison JM, Akitake CM, Goll MG, Rhee JM, Gosse N, Baier H, Halpern ME, Leach SD, Parsons MJ (2007) Transactivation from Gal4-VP16 transgenic insertions for tissue-specific cell labeling and ablation in zebrafish. Dev Biol 304:811–824. CrossRef Medline

El Marroun H, White TJ, van der Knaap NJ, Homberg JR, Fernández G, Schoemaker NK, Jaddoe VW, Hofman A, Verhulst FC, Hudziak JJ, Stricker BH, Tiemeier H (2014) Prenatal exposure to selective serotonin reuptake inhibitors and social responsiveness symptoms of autism: population-based study of young children. Br J Psychiatry 205:95–102. CrossRef Medline

Evans TA, Bashaw GJ (2010) Axon guidance at the midline: of mice and flies. Curr Opin Neurobiol 20:79–85. CrossRef Medline

Gidaya NB, Lee BK, Burstyn I, Yudell M, Mortensen EL, Newschaffer CJ (2014) In utero exposure to selective serotonin reuptake inhibitors and risk for autism spectrum disorder. J Autism Dev Disord 44:2558–2567. CrossRef Medline

Gingrich JA, Ansorge MS, Merker R, Weisstaub N, Zhou M (2003) New lessons from knockout mice: The role of serotonin during development and its possible contribution to the origins of neuropsychiatric disorders. CNS Spectr 8:572–577. Medline

Hancock ML, Preitner N, Quan J, Flanagan JG (2014) MicroRNA-132 is enriched in developing axons, locally regulates Rasa1 mRNA, and promotes axon extension. J Neurosci 34:66–78. CrossRef Medline

Hanson MG, Landmesser LT (2004) Normal patterns of spontaneous activity are required for correct motor axon guidance and the expression of specific guidance molecules. Neuron 43:687–701. CrossRef Medline

Harrington RA, Lee LC, Crum RM, Zimmerman AW, Hertz-Picciotto I (2013) Serotonin hypothesis of autism: implications for selective serotonin reuptake inhibitor use during pregnancy. Autism Res 6:149–168. CrossRef Medline

Hay-Schmidt A (2000) The evolution of the serotonergic nervous system. Proc Biol Sci 267:1071–1079. CrossRef Medline

Imondi R, Kaprielian Z (2001) Commissural axon pathfinding on the contralateral side of the floor plate: a role for B-class ephrins in specifying the dorsoventral position of longitudinally projecting commissural axons. Development 128:4859–4871. Medline

Jao LE, Wente SR, Chen W (2013) Efficient multiplex biallelic zebrafish genome editing using a CRISPR nuclease system. Proc Natl Acad Sci U S A 110:13904–13909. CrossRef Medline

Jassen AK, Yang H, Miller GM, Calder E, Madras BK (2006) Receptor regulation of gene expression of axon guidance molecules: implications for adaptation. Mol Pharmacol 70:71–77. Medline

Jinek M, Chylinski K, Fonfara I, Hauer M, Doudna JA, Charpentier E (2012) A programmable dual-RNA-guided DNA endonuclease in adaptive bacterial immunity. Science 337:816–821. CrossRef Medline

Jitsuki S, Takemoto K, Kawasaki T, Tada H, Takahashi A, Becamel C, Sano A, Yuzaki M, Zukin RS, Ziff EB, Kessels HW, Takahashi T (2011) Serotonin mediates cross-modal reorganization of cortical circuits. Neuron 69:780–792. CrossRef Medline

Jung H, O'Hare CM, Holt CE (2011) Translational regulation in growth cones. Curr Opin Genet Dev 21:458–464. CrossRef Medline

Kadison SR, Mäkinen T, Klein R, Henkemeyer M, Kaprielian Z (2006) EphB receptors and ephrin-B3 regulate axon guidance at the ventral midline of the embryonic mouse spinal cord. J Neurosci 26:8909–8914. CrossRef Medline

Kaplan BB, Kar AN, Gioio AE, Aschrafi A (2013) MicroRNAs in the axon and presynaptic nerve terminal. Front Cell Neurosci 7:126. Medline

Kaslin J, Panula P (2001) Comparative anatomy of the histaminergic and other aminergic systems in zebrafish (Danio rerio). J Comp Neurol 440:342–377. CrossRef Medline

Katz LC, Shatz CJ (1996) Synaptic activity and the construction of cortical circuits. Science 274:1133–1138. CrossRef Medline

Kettleborough RN, Busch-Nentwich EM, Harvey SA, Dooley CM, de Bruijn E, van Eeden F, Sealy I, White RJ, Herd C, Nijman IJ, Fényes F, Mehroke S, Scahill C, Gibbons R, Wali N, Carruthers S, Hall A, Yen J, Cuppen E, Stemple DL (2013) A systematic genome-wide analysis of zebrafish protein-coding gene function. Nature 496:494–497. CrossRef Medline

Kuzelova H, Ptacek R, Macek M (2010) The serotonin transporter gene (5-HTT) variant and psychiatric disorders: review of current literature. Neuro Endocrinol Lett 31:4–10. Medline

Lambert AM, Bonkowsky JL, Masino MA (2012) The conserved dopaminergic diencephalospinal tract mediates vertebrate locomotor development in zebrafish larvae. J Neurosci 32:13488–13500. CrossRef Medline

Lesch KP, Waider J (2012) Serotonin in the modulation of neural plasticity and networks: implications for neurodevelopmental disorders. Neuron 76:175–191. CrossRef Medline

Lillesaar C (2011) The serotonergic system in fish. J Chem Neuroanat 41:294–308. CrossRef Medline

Lillesaar C, Stigloher C, Tannhäuser B, Wullimann MF, Bally-Cuif L (2009) Axonal projections originating from raphe serotonergic neurons in the

developing and adult zebrafish, Danio rerio, using transgenics to visualize raphe-specific pet1 expression. J Comp Neurol 512:158–182. CrossRef Medline

Link V, Shevchenko A, Heisenberg CP (2006) Proteomics of early zebrafish embryos. BMC Dev Biol 6:1. CrossRef Medline

Martin KC, Casadio A, Zhu H, Yaping E, Rose JC, Chen M, Bailey CH, Kandel ER (1997) Synapse-specific, long-term facilitation of *Aplysia* sensory to motor synapses: a function for local protein synthesis in memory storage. Cell 91:927–938. CrossRef Medline

Matsukawa M, Nakadate K, Ishihara I, Okado N (2003) Synaptic loss following depletion of noradrenaline and/or serotonin in the rat visual cortex: a quantitative electron microscopic study. Neuroscience 122: 627–635. CrossRef Medline

McFadden LM, Carter S, Matuszewich L (2012) Juvenile exposure to methamphetamine attenuates behavioral and neurochemical responses to methamphetamine in adult rats. Behav Brain Res 229:118–122. CrossRef Medline

McLean DL, Fetcho JR (2004) Ontogeny and innervation patterns of dopaminergic, noradrenergic, and serotonergic neurons in larval zebrafish. J Comp Neurol 480:38–56. CrossRef Medline

Miniaci MC, Kim, JH, Puthanveettil SV, Si K, Zhu H, Kandel ER, Bailey CH (2008) Sustained CPEB-dependent local protein synthesis is required to stabilize synaptic growth for persistence of long-term facilitation in *Aplysia*. Neuron 59:1024–1036. CrossRef Medline

Nakagawa S, Brennan C, Johnson KG, Shewan D, Harris WA, Holt CE (2000) Ephrin-B regulates the Ipsilateral routing of retinal axons at the optic chiasm. Neuron 25:599–610. CrossRef Medline

Pasquale EB (2008) Eph-ephrin bidirectional signaling in physiology and disease. Cell 133:38–52. CrossRef Medline

Persico AM, Mengual E, Moessner R, Hall FS, Revay RS, Sora I, Arellano J, DeFelipe J, Gimenez-Amaya JM, Conciatori M, Marino R, Baldi A, Cabib S, Pascucci T, Uhl GR, Murphy DL, Lesch KP, Keller F, Hall SF (2001) Barrel pattern formation requires serotonin uptake by thalamocortical afferents, and not vesicular monoamine release. J Neurosci 21:6862–6873. Medline

Pisharath H, Parsons MJ (2009) Nitroreductase-mediated cell ablation in transgenic zebrafish embryos. Methods Mol Biol 546:133–143. CrossRef Medline

Pocock R, Hobert O (2010) Hypoxia activates a latent circuit for processing gustatory information in *C. elegans*. Nat Neurosci 13:610–614. CrossRef Medline

Polleux F, Ince-Dunn G, Ghosh A (2007) Transcriptional regulation of vertebrate axon guidance and synapse formation. Nat Rev Neurosci 8:331–340. Medline

Prasad HC, Steiner JA, Sutcliffe JS, Blakely RD (2009) Enhanced activity of human serotonin transporter variants associated with autism. Philos Trans R Soc Lond B Biol Sci 364:163–173. CrossRef Medline

Puthanveettil SV, Monje FJ, Miniaci MC, Choi, YB, Karl KA, Khandros E, Gawinowicz MA, Sheetz MP, Kandel ER (2008) A new component in synaptic plasticity: upregulation of kinesin in the neurons of the gill-withdrawal reflex. Cell 135:960–973. CrossRef Medline

Rahman MS, Thomas P (2009) Molecular cloning, characterization and expression of two tryptophan hydroxylase (TPH-1 and TPH-2) genes in the hypothalamus of Atlantic croaker: down-regulation after chronic exposure to hypoxia. Neuroscience 158:751–765. CrossRef Medline

Rai D, Lee BK, Dalman C, Golding J, Lewis G, Magnusson C (2013) Parental depression, maternal antidepressant use during pregnancy, and risk of autism spectrum disorders: population based case-control study. BMJ 346:f2059. CrossRef Medline

Riccio O, Potter G, Walzer C, Vallet P, Szabó G, Vutskits L, Kiss JZ, Dayer AG (2009) Excess of serotonin affects embryonic interneuron migration through activation of the serotonin receptor 6. Mol Psychiatry 14:280–290. CrossRef Medline

Rubenstein JL (1998) Development of serotonergic neurons and their projections. Biol Psychiatry 44:145–150. Medline

Saxena PR (1995) Serotonin receptors: subtypes, functional responses and therapeutic relevance. Pharmacol Ther 66:339–368. CrossRef Medline

Schneider H, Fritzky L, Williams J, Heumann C, Yochum M, Pattar K, Noppert G, Mock V, Hawley E (2012) Cloning and expression of a zebrafish 5-HT(2C) receptor gene. Gene 502:108–117. CrossRef Medline

Severson CA, Wang W, Pieribone VA, Dohle CI, Richerson GB (2003) Midbrain serotonergic neurons are central pH chemoreceptors. Nat Neurosci 6:1139–1140. CrossRef Medline

Silberstein SD (1998) Methysergide. Cephalalgia 18:421–435. CrossRef Medline

Son JH, Latimer C, Keefe KA (2011) Impaired formation of stimulus-response, but not action-outcome, associations in rats with methamphetamine-induced neurotoxicity. Neuropsychopharmacology 36:2441–2451. CrossRef Medline

Steinbusch HW (1981) Distribution of serotonin-immunoreactivity in the central nervous system of the rat-cell bodies and terminals. Neuroscience 6:557–618. CrossRef Medline

Stevenson TJ, Trinh T, Kogelschatz C, Fujimoto E, Lush ME, Piotrowski T, Brimley CJ, Bonkowsky JL (2012) Hypoxia disruption of vertebrate CNS pathfinding through ephrinB2 Is rescued by magnesium. PLoS Genet 8:e1002638. CrossRef Medline

Suárez R, Fenlon LR, Marek R, Avitan L, Sah P, Goodhill GJ, Richards LJ (2014) Balanced interhemispheric cortical activity is required for correct targeting of the corpus callosum. Neuron 82:1289–1298. CrossRef Medline

Suli A, Mortimer N, Shepherd I, Chien CB (2006) Netrin/DCC signaling controls contralateral dendrites of octavolateralis efferent neurons. J Neurosci 26:13328–13337. CrossRef Medline

Sutcliffe JS, Delahanty RJ, Prasad HC, McCauley JL, Han Q, Jiang L, Li C, Folstein SE, Blakely RD (2005) Allelic heterogeneity at the serotonin transporter locus (SLC6A4) confers susceptibility to autism and rigid-compulsive behaviors. Am J Hum Genet 77:265–279. CrossRef Medline

Taylor AC, Mendel TA, Mason KE, Degen KE, Yates PA, Peirce SM (2012) Attenuation of ephrinB2 reverse signaling decreases vascularized area and preretinal vascular tuft formation in the murine model of oxygen-induced retinopathy. Invest Ophthalmol Vis Sci 53:5462–5470. CrossRef Medline

Teraoka H, Russell C, Regan J, Chandrasekhar A, Concha ML, Yokoyama R, Higashi K, Take-Uchi M, Dong W, Hiraga T, Holder N, Wilson SW (2004) Hedgehog and Fgf signaling pathways regulate the development of tphR-expressing serotonergic raphe neurons in zebrafish embryos. J Neurobiol 60:275–288. CrossRef Medline

Toda T, Homma D, Tokuoka H, Hayakawa I, Sugimoto Y, Ichinose H, Kawasaki H (2013) Birth regulates the initiation of sensory map formation through serotonin signaling. Dev Cell 27:32–46. CrossRef Medline

Turlejski K (1996) Evolutionary ancient roles of serotonin: long-lasting regulation of activity and development. Acta Neurobiol Exp (Wars) 56:619–636. Medline

van Kleef ES, Gaspar P, Bonnin A (2012) Insights into the complex influence of 5-HT signaling on thalamocortical axonal system development. Eur J Neurosci 35:1563–1572. Medline

Vitalis T, Cases O, Passemard S, Callebert J, Parnavelas JG (2007) Embryonic depletion of serotonin affects cortical development. Eur J Neurosci 26:331–344. CrossRef Medline

Wan Y, Otsuna H, Chien C-B, Hansen C (2012) FluoRender: an application of 2D image space methods for 3D and 4D confocal microscopy data visualization in neurobiology research. IEEE Pac Vis Symp 201–208.

Wang W, Feng L, Zhang H, Hachy S, Satohisa S, Laurent LC, Parast M, Zheng J, Chen DB (2012) Preeclampsia up-regulates angiogenesis-associated microRNA (i.e., miR-17, -20a, and -20b) that target ephrin-B2 and EPHB4 in human placenta. J Clin Endocrinol Metab 97:E1051–E1059. CrossRef Medline

Wilson SW, Ross LS, Parrett T, Easter SS Jr (1990) The development of a simple scaffold of axon tracts in the brain of the embryonic zebrafish, *Brachydanio rerio*. Development 108:121–145. Medline

Winckler B, Mellman I (2010) Trafficking guidance receptors. Cold Spring Harb Perspect Biol 2:a001826. Medline

Witteveen JS, Middelman A, van Hulten JA, Martens GJ, Homberg JR, Kolk SM (2013) Lack of serotonin reuptake during brain development alters rostral raphe-prefrontal network formation. Front Cell Neurosci 7:143. Medline

Xing L, Hoshijima K, Grunwald DJ, Fujimoto E, Quist TS, Sneddon J, Chien CB, Stevenson TJ, Bonkowsky JL (2012) Zebrafish foxP2 zinc finger nuclease mutant has normal axon pathfinding. PLoS One 7:e43968. CrossRef Medline

Xing L, Quist TS, Stevenson TJ, Dahlem TJ, Bonkowsky JL (2014) Rapid and efficient zebrafish genotyping using PCR with high-resolution melt analysis. J Vis Exp e51138.

Yokogawa T, Hannan MC, Burgess HA (2012) The dorsal raphe modulates sensory responsiveness during arousal in zebrafish. J Neurosci 32:15205–15215. CrossRef Medline